Crosstalk between Rac and Rap GTPases in migrating cells

Dissertation

zur Erlangung des akademischen Grades des Doktors der Naturwissenschaften (Dr. rer. nat.) an der Fakultät Chemie und Chemische Biologie der Technischen Universität Dortmund

vorgelegt von

Ricarda Lüttig

geboren am 13.09.1997 in Holzminden

im September 2025 in Dortmund

IMPRS
for Living Matter
INTERNATIONAL MAX PLANCK
RESEARCH SCHOOL

technische universität
dortmund

First examiner: Priv.-Doz. Dr. Leif Dehmelt
Second examiner: Prof. Dr. med. Jan G. Hengstler

The work presented in this thesis was performed in the group of Priv.-Doz. Dr. Leif Dehmelt in the Faculty of Chemistry and Chemical Biology, TU Dortmund University, Germany.

Acknowledgements

First, I would like to thank Leif for letting me complete my PhD Thesis in his working group and fully supporting and mentoring me throughout this journey. I am incredibly grateful that I got to continue this exciting project and was allowed the necessary space and support for me to grow. Having a supervisor that believes in you and confidently guides you with an open ear and open-door policy really made this PhD not only another degree to complete, but 3 wonderful years that I will always keep in good memory. It is not self-evident to have such a great and dedicated mentor!

I would also like to thank Prof. Dr. med. Jan G. Hengstler, who kindly took over the position of my second examiner for taking the time and effort to guide my thesis.

Another big thank you goes towards the IMPRS. Being part of such a community was great from a personal as well as scientific perspective. Special thanks go to the wonderful coordinators Christa and Lucia, for their warm welcome, great teamwork with the representatives and constant support.
I would also like to express my gratitude to Prof. Dr. Perihan Nalbant and Prof. Dr. Daniel Summerer who made up my Thesis Advisory Committee and took the time to guide my thesis progress.

I would also like to thank the lab of Dr. Perihan Nalbant, for scientific discussions as well as many nice hours spent at shared Christmas parties and BBQ get-togethers. I will miss the world's best margarita cocktails (peer reviewed) and culinary excursions!

Another big thank you goes to the whole Dehmelt Lab, especially my current lab mates Caro, Arya and Luisa, as well as my former lab mates Suchet and Haritha. Caro and Suchet had a big part in helping me get my thesis started and working with them allowed me to learn a lot, especially concerning microscope operation, image analysis and experimental setups. This last year of our PhDs was incredibly fast and eventful, yet we managed to maintain a great lab culture and supported and uplifted each other during stressful times. It was a pleasure spending time with you in and out of lab and I am grateful we quickly became good friends along the way!

I would also like to thank everyone from the TU Dortmund, especially the working group of Prof. Dr. Summerer, for many wonderful hours spend in and out of lab and so many great friendships emerging along the way!

I would also like to thank everyone from Department 2, especially the late Philippe Bastiaens, for departmental support, helpful discussions and the organization of many successful practical courses. I would also like to thank Sven Müller for expert microscopy support.

Finally, my biggest thank you goes to my parents Ferdi and Bärbel, my brother Lennart, my family and my friends for their loving support during the time of this PhD. Completing a doctoral degree always comes with highs and lows and I wouldn´t have made it without you!

Table of Contents

The contents of chapters 3.1 (incl all subchapters), 4, 6.1, 6.2.1, 6.2.2, 6.3 (excl. subchapter 6.3.5) and 8.2.2 have been previously published in Lüttig et al. (2025):

Lüttig, R., Nanda, S., Chandran, Haritha T., Dehmelt, L., (**2025**). Crosstalk between Rac and Rap GTPases in migrating cells. *Molecular Biology of the Cell*. https://doi.org/10.1091/MBC.E25-02-0058.

I List of Abbreviations

ADP	adenosine diphosphate
ATP	adenosine triphosphate
ECM	extracellular matrix
ERMs	ezrin-radixin-moesin proteins
FA	focal adhesion
FAK	focal adhesion kinase
FERM	4.1-ezrin-radixin-moesin
GAP	GTPase activating protein
GBD	GTPase binding domain
GDI	guanosine nucleotide dissociation inhibitor
GDP	guanosine diphosphate
GEF	guanine nucleotide exchange factor
GTP	guanosine triphosphate
LOV	light oxygen voltage
MAP	molecular activity painting
MAPK	mitogen-activated protein kinase
MAP4K4	mitogen-activated protein kinase kinase kinase kinase 4
NMII	non-muscle myosin II
PA-Rac1	photoactivatable Rac1
Scar	suppressor of cAR, i.e. of cyclic AMP receptors
TIRF-M	total internal reflection fluorescence microscopy
WASP	Wiskott-Aldrich syndrome protein

II Abstract

Cell migration is a process involved in various physiological and pathophysiological processes, including immune cell migration and cancer metastasis. Efficient cell migration requires precise spatio-temporal coordination of several fundamental cell biological processes, in particular of cell protrusion, adhesion and retraction. Signal proteins of the Rho and Ras/ Rap family GTPases are thought to be master regulators of these fundamentally important processes, and direct investigations of these proteins in living cells is therefore expected to aid our understanding, how they are coordinated in space and time. Here, highly sensitive, effector-domain based activity sensors for Ras, Rac1 and Rap, were used in combination with both long-term and short-term activity perturbations to investigate the signal network that controls cell migration. In the keratinocyte-derived A431 cancer cell line, Rac activity was already known to correlate tightly with local cell protrusions. In this thesis, Rap activity was observed already before Rac activity and remained elevated for a prolonged time after the actual protrusion event. The combination of activity measurements with rapid optogenetic perturbations revealed a clear hierarchy, in which Rap can efficiently and unidirectionally activate Rac. This suggests an instructive role of the Rap GTPase in the generation of newly formed protrusions. Rap GTPases were already known to regulate cellular adhesion, and their prolonged activity after cell protrusion further supports this idea. Further functional investigations into the role of distinct Rap isoforms suggested that the two major isoforms Rap1a and Rap2b have an antagonistic effect on cell adhesion. While knockdown of Rap1a resulted in decreased cell adhesion, knockdown of Rap2b had the opposite effect. Taken together, these studies suggest that a unidirectional activity crosstalk couples Rap activity to Rac activity to induce cellular protrusion, and that prolonged Rap activity after cell protrusion regulates cell adhesion.

III Zusammenfassung

Zellmigration spielt eine zentrale Rolle in zahlreichen physiologischen und patho-physiologischen Prozessen, beispielsweise der zielgerichteten Wanderung von Immunzellen oder der Metastasierung von Tumorzellen. In diesem Prozess spielt die präzise zeitliche und räumliche Koordination verschiedener fundamentaler zellbiologischer Prozesse, wie der gerichteten Bildung von Ausstülpungen, der Zelladhäsion und der Zellkontraktion eine wichtige Rolle. Signalproteine der Rho und Ras/Rap Familien kleiner GTPasen spielen in dieser Koordination eine wichtige Rolle. Die direkte Untersuchung ihrer dynamischen Aktivität und ihrer Wechselwirkungen in lebenden Zellen ist entscheidend, um die zugrunde liegenden Mechanismen dieser Koordination besser zu verstehen. In dieser Arbeit wurden hochsensitive Aktivitätssensoren für die wichtigsten Vertreter dieser Signalproteine, Ras, Rac1 und Rap eingesetzt. In Kombination mit kurz- und langfristigen Aktivitätsstörungen konnten zentrale Eigenschaften der regulatorischen Netzwerke aufgedeckt werden, welche die Aktivitäten dieser Signalproteine miteinander verbinden. In der von Keratinozyten abgeleiteten Krebszelllinie A431 wurde bereits eine enge Korrelation der Rac-Aktivität mit lokalen Zellausstülpungen beobachtet. In dieser Arbeit konnte gezeigt werden, dass Rap vor, während und auch noch über einen längeren Zeitraum nach Rac-vermittelten Zellausstülpungen aktiv ist. Durch eine Kombination von Aktivitätsmessungen mit schnellen optogenetischen Störungen wurde eine unidirektionale Kausalität zwischen diesen Signalproteinen nachgewiesen, durch welche Rac effizient durch Rap aktiviert wird. Dies weist auf eine instruktive Rolle von Rap GTPasen bei der Initiierung neuer Zellausstülpungen hin. Die beobachtete verlängerte Rap-Aktivität nach der initialen Zellausstülpung unterstützt vorherige Studien, welche eine Rolle von Rap in der Zelladhäsion beschrieben haben. Funktionelle Analysen spezifischer Rap-Isoformen deuten darauf hin, dass Rap1a und Rap2b antagonistische Effekte auf die zelluläre Adhäsion haben: Der Knockdown von Rap1a führte zu einer verminderten Adhäsion, während der Knockdown von Rap2b das Gegenteil bewirkte. Zusammenfassend zeigen diese Ergebnisse, dass eine unidirektionale Verknüpfung die Rap- und Rac-Aktivität koppelt und damit die Bildung zellulärer Protrusionen initiiert, und dass die verlängerte Rap-Aktivität nach einer neuen Zellausstülpung die Ausbildung neuer Adhäsionen reguliert.

1 Introduction

1.1 (Patho-)physiological relevance of cell migration

Cell migration plays an important role in numerous physiological and pathological processes. Starting already during embryonic development, directed and collective migration of cells is vital to ensure the proper formation of tissues and organs (Horwitz & Webb, 2003). While homeostatic processes such as inflammation-induced immune cell migration or restoration of structural damage to tissues are nature´s precautions to maximize chances of survival, aberrant cell migration has clear implications for diseases and their progression (Grada et al., 2017; Luster et al., 2005). The most prominent example, describing a major hallmark of cancer, is the invasion of foreign tissues by malignant cancer cells, resulting in metastases (Hanahan, 2022). Such tumor cells, most often subject to genetic abnormalities, leave the primary site as a response to various parameters, e.g. hypoxia or lack of nutrients, by exhibiting dysregulated migratory behavior, and often enhanced migration efficiency. Exemplarily, former non-motile epithelial cells develop a motile phenotype, allowing cell dissemination and ultimately, cancer metastasis (Alexandrova et al., 2020; Novikov et al., 2020).

1.2 Cell biological mechanism of cell migration

1.2.1 Modes of cell migration

In two-dimensional systems, various patterns of cell migration have been described. In particular, cells can either migrate in a persistent, directional mode, or via an intrinsically random, more exploratory mode. Interestingly, dynamic switching between these modes by various triggers has also been described (Ipiña et al., 2023; Pankov et al., 2005). The exploratory cell migration mode is characterized by distinct changes in the plasma membrane shape, in particular by coupled, highly dynamic cycles of cell protrusion and cell retraction. In the highly motile amoeboid migration mode, these dynamics are exhibited transiently towards all directions, with no detectable polarization of the cell at any given time, while in typical mesenchymal cell migration, these protrusion and retraction events appear mainly in the front of the cell and the back of the cells shows net retraction (Nalbant & Dehmelt, 2018; Seetharaman & Etienne-Manneville, 2020). The exploratory migration mode, with frequent changes in direction, is a central feature of any immune cells, which patrol randomly in search of antigens (Moreau et al., 2018). In contrast, directed cell migration is defined by a more

stable spatial segregation of locally persistent front protrusion and net rear retraction and typically associated with a strongly polarized cell morphology (Nalbant & Dehmelt, 2018). Such a migration mode is famously seen in primary fish epidermal keratocytes (Euteneuer & Schliwa, 1984), and is critical for many processes, such as the active immune response towards a target site (Horwitz & Webb, 2003; Moreau et al., 2018; Niculescu et al., 2015).

Naturally, cells are permanently subjected to the presence of multifaceted external cues, often guiding directed cell migration by the concentration of soluble and diffusible chemical substances (chemotaxis), surface bound extracellular matrix (ECM) components (haptotaxis), light (phototaxis) or electrical fields (galvanotaxis) (Aznavoorian et al., 1990; Sunyer & Trepat, 2020). Additionally, mechanical cues such as stiffness gradients in the ECM can influence cell migration directionality (durotaxis) (De Pascalis & Etienne-Manneville, 2017). Such influences on directional migration are of high physiological relevance, as for example secretion of ECM proteins like fibronectin or collagen can tune macrophage activity (Stinson et al., 2024). In the absence of external cues, many cells actively exhibit random migration to again find spatial cues to guide them (Bosgraaf & Van Haastert, 2009), but some cell types, such as the primary fish epidermal keratocytes, and even small, denucleated fragments of these cells, can still migrate directionally and persistently in the absence of external cues (Euteneuer & Schliwa, 1984).

Opposed to individual, single cell motility, seen for example in leukocytes of the immune system, collective migration of many cells within a tissue is critical for events like wound healing, reepithelialization or major embryonic tissue reorganizations (Alanko et al., 2023; Niculescu et al., 2015; Scarpa & Mayor, 2016). During collective migration, multiple cells move in a coordinated fashion, while they retain cell-cell contacts, thereby promoting both active and passive cell translocation (Friedl & Gilmour, 2009).

1.2.2 Steps in the migration of individual, single cells

During migration, cells have to coordinate a variety of different processes. In a first step, the leading edge is extended as the cell forms a protrusion, pushing the front of the cell forward. Subsequently, new contacts to the external matrix are formed and new adhesions are generated in the anterior region of the cell, stabilizing the newly formed protrusion. Simultaneously, the cytoplasm contracts, as stress fibers linked to these adhesions generate contractile forces. After disassembly of adhesions in the back of the cell, these contractile forces drive the cell retraction (Friedl & Wolf, 2009; Sheetz et al., 1999). This release from contact sites generates excess dorsal surface, allowing the formation of new front protrusions (Trepat et al., 2012). Iterative repetitions of these protrusion, adhesion and retraction events, sometimes even occurring simultaneously, allow efficient cell migration (Doyle & Lee, 2005; Friedl & Wolf, 2009).

1.3 Molecular mechanisms in cell migration

1.3.1 Protrusive forces generated by actin polymerisation

The dynamic cell shape changes that drive cell migration depend on specialized structures that are collectively called the cytoskeleton. The cytoskeleton serves two major functions in these processes: First, it acts as an internal structural framework, providing cells with a scaffold to stabilize and maintain their shape, and second, it is constantly rearranged by pulling and pushing forces to actively deform their shape. In particular, during migration, cells have to undergo dramatic morphological changes in order to successfully navigate through physical barriers within the ECM or even just crawl on a flat surface. These shape-changes require precisely regulated cytoskeletal rearrangements (Cooper, 2000; Holle et al., 2019; Wollrab et al., 2019). It is now well-understood, that protrusion generating forces are primarily exerted by actin networks that polymerize and push against the leading edge of migrating cells. These actin dynamics are well described by the dendritic nucleation model, illustrating this force generation by the formation of branched actin structures after their nucleation by Arp2/3 (Figure 1) (Miller, 2002; Nicholson-Dykstra et al., 2005).

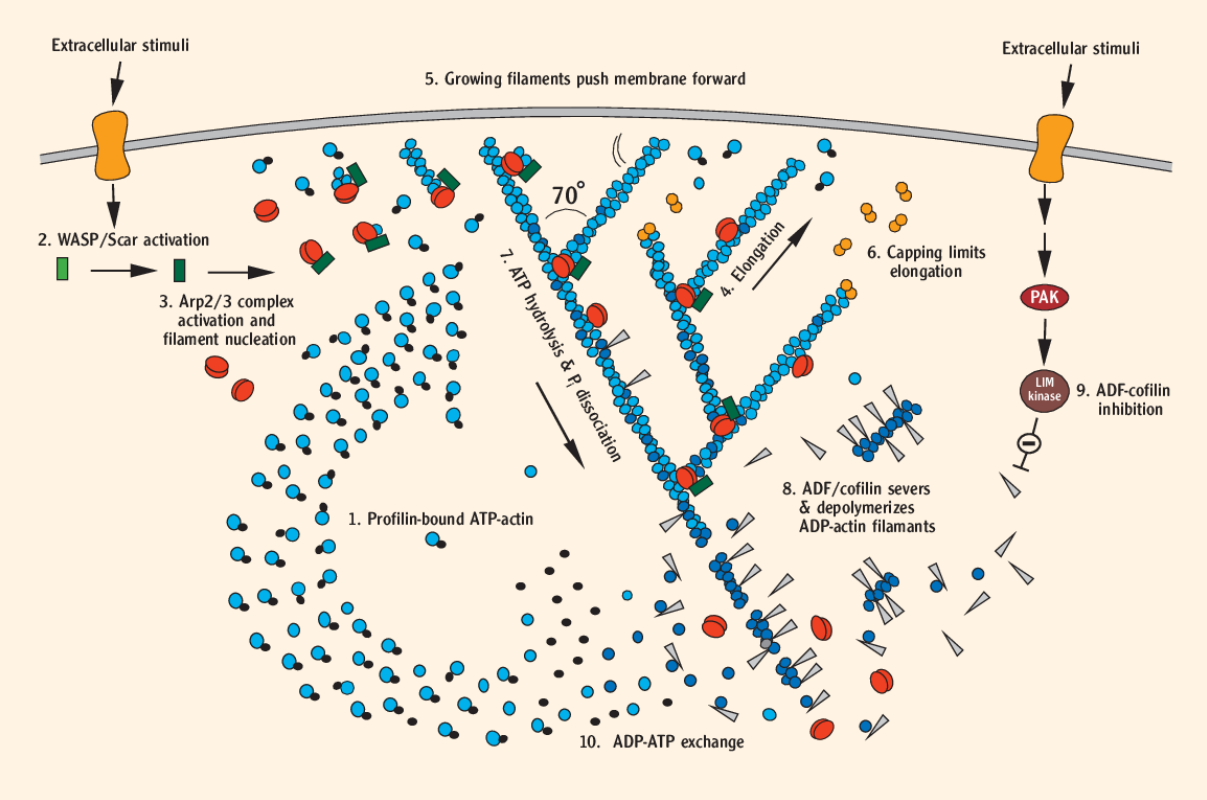

Figure 1: The dendritic nucleation model. Based on this model, the force-generating actin polymerization is based on a cyclic process, which starts with profilin-bound ATP-actin molecules (step 1), the principal source of monomeric actin for filament polymerization. Profilin is fundamentally regulating actin polymerization by facilitating the exchange of actin-bound adenosine diphosphate (ADP) to adenosine triphosphate (ATP), preventing spontaneous *de novo* polymerization of monomers and aiding polymerization onto existing filaments (Y. Li et al., 2008). Upon receival of extracellular stimuli, proteins of the WASP/Scar family, in particular the WAVE regulatory complex (WRC) are activated (step 2), in turn activating the actin filament nucleating complex Arp2/3 (step 3) (Bear et al., 1998; Vignjevic et al., 2003). Subsequently, actin monomers polymerize (step 4), elongating new and previously existing filaments, creating a branched network (Pollard et al., 2001). These growing filaments can then push the membrane forward by a Brownian ratchet mechanism (step 5), in which a polymerization-driven force is generated by continuous assembly of actin monomers, which is enabled by membrane fluctuations and filament elasticity (Ananthakrishnan & Ehrlicher, 2007). Elongation is limited by capping proteins, that bind barbed-ends of filamentous actin, preventing further polymerization (step 6). This step is crucial to ensure network stability, as it keeps individual filaments short (Mejillano et al., 2004). In the polymerized form, ATP hydrolysis and P_i dissociation are stimulated within actin (step 7), and subsequently, ADF/cofilin severs the ADP-actin filaments, facilitating their depolymerization and accelerating treadmilling (step 8) (Theriot, 1997). ADF/cofilin inhibition by the LIM kinase is again regulated by external stimuli (step 9). Exchange of ADP to ATP and thereby recycling of monomers completes the cycle (step 10) (Pollard et al., 2001). Figure source: Pollard et al., 2001.

At the leading edge of migrating cells, the actin machinery can generate distinct forms of actin-based protrusion. Fan-like Lamellipodia, best described by the dendritic nucleation model, facilitate persistent surface-level protrusions, while finger-like filopodia allow sensitive exploration of the cell's environment (Mejillano et al., 2004). Such filopodial protrusions are described to protrude from the branched actin network inside the mammalian lamellipod (convergent elongation model (Svitkina et al., 2003)) or *de novo* nucleate at amoeba filopodial tips in a formin-dependent fashion (*de novo* nucleation model (Medalia et al., 2007)). Within filopodia, parallel actin filaments are clustered and continuously elongated without capping or branching; capping protection being mediated by tip-complex proteins (Mejillano et al., 2004). Stiff bundling of core actin filaments is achieved by incorporation of crosslinking fascin proteins (Mattila & Lappalainen, 2008).

While filopodial structures mainly serve the purpose of sensing the environment, fan-like lamellipodia are an integral part of basic cell migration (Lundquist, 2009). After extending the leading edge of the cell, new contacts with the matrix are made, which need to be established as cellular adhesions in a next step, stabilizing the newly formed protrusion (Michaelis, 2014).

1.3.2 Cell adhesion by integrin receptors

To efficiently migrate, cells need to be able to generate traction against their substrate. To enable this traction and local force transmission, cells have to precisely control the assembly and disassembly of tight adhesion points that link force generation by the actin cytoskeleton to the extracellular matrix (EMC). This linkage is mediated by specialized structures, the so-called focal adhesions (FAs), in which transmembrane receptors are linked to multiple layers of regulatory proteins that participate in mechano-sensitive interactions (Figure 2) (Case & Waterman, 2015).

During protrusion, heterodimeric transmembrane receptors of the integrin family bind to ECM ligands like fibronectin via their extracellular domains and/or to cytoplasmic proteins like talin via their intracellular domains (Trepat et al., 2012). These interactions mediate ´outside-in´ and ´inside-out´-signaling to control the activity state of the integrin receptors and the associated proteins in the focal adhesions. Mechanical signals can then induce conformational changes of the α and β integrin tails, and the exposed domains then allow high-affinity binding on both sides of the integrin (Case &

Waterman, 2015). Maturation of the newly forming, nascent focal adhesion (FA) at the lamellipodium base requires coupling to the actin cytoskeleton and tension either by myosin-mediated contraction or extracellular pulling (Alpha et al., 2020; Geiger et al., 2009; Pasapera et al., 2010; Wehrle-Haller, 2013). Specifically, mechanosensory proteins within the FAs, like talin and vinculin, undergo force-dependent stretching and unfolding, reinforcing their binding of integrins with their 4.1-ezrin-radixin-moesin (FERM) domains, triggering integrin clustering and thereby facilitating the continuous remodeling of the actin-integrin interplay (Alpha et al., 2020; Jansen et al., 2017). While α-actinin crosslinks actin filaments that attach to the FAs, structural proteins like paxillin act as stabilizing scaffolds within FAs (Alpha et al., 2020; Geiger et al., 2009).

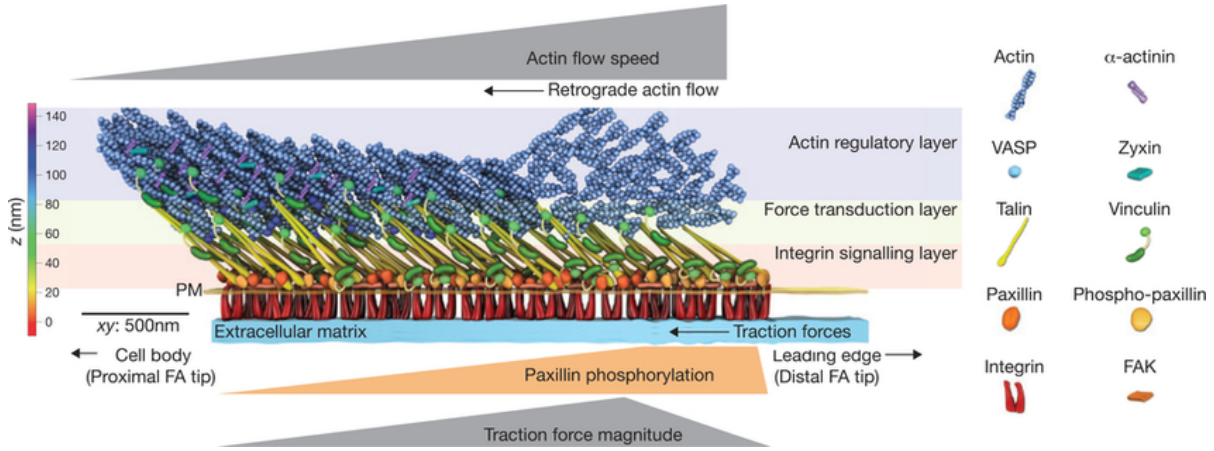

Figure 2: Architecture of focal adhesions at the end of stress fibers. The schematic shows a structural model based on nanoscopic imaging that illustrates the layered organization of core components of focal adhesions and how they are involved in mechanical force transduction. Immediately above the transmembrane integrins, the integrin signaling layer is composed of cytoplasmic integrin tails interacting with paxillin, the focal adhesion kinase (FAK) and the head-domain of talin. Right above these components that are predominantly involved in signaling is the force transduction layer, which consists of mechanosensory proteins like vinculin and talin. This layer connects the integrin signaling layer to the actin regulatory layer, which links the FA to stress fibers bound to α-actinin, VASP and zyxin. Figure source: Case & Waterman, 2015.

1.3.3 Contractile forces generated by actomyosin

In addition to protruding forces, motile cells also generate contractile forces to increase tension towards their substrate and to mediate cell retraction. These contractile forces rely on the interplay between actin filaments and molecular motors based on non-muscle myosin II (NMII). Actin filaments are polar and have structurally distinct filament ends, the so-called barbed (+) and pointed (-) ends. In migratory, non-muscle cells, the myosin-based motors are also organized into multimeric, antiparallel minifilaments, in

which the motor head groups point to both filament ends, and the tails are kept together in their center. This bipolar setup of myosin minifilaments allows them to slide antiparallel actin filaments against each other, thereby shortening antiparallel arrangements of actin filaments, leading to their contraction and generating a pulling force (Wollrab et al., 2019).

1.4 Spatio-temporal coordination of cell shape changes and adhesion in cell migration

1.4.1 General concepts

The precise spatio-temporal coordination of cell protrusion, adhesion and retraction/ contraction is critical to facilitate efficient cell migration (Nanda et al., 2023). This coordination is thought to be mediated by activity crosstalk between regulators that control these distinct cell biological processes (Bar-Sagi & Hall, 2000). Positive and negative feedback regulators play critical roles in this context, as they can generate activity patterns to organize and coordinate these processes in space and time (Graessl et al., 2017). In particular, such feedback regulators were proposed to be involved in the generation of dynamic cell contraction pulses, in dynamic protrusion-retraction cycles in exploratory cell migration, or the stabilization of front-rear polarity in directional migration (Devreotes et al., 2017; Gandalovičová et al., 2016; Graessl et al., 2017; Nanda et al., 2023). In particular, small GTPases of the Rho and Ras/Rap families were shown to be key regulators of cell protrusion, adhesion and retraction/ contraction (Nanda et al., 2023; Raaijmakers & Bos, 2009).

1.4.2 Molecular mechanisms

Signal proteins of the small GTPase family were found to be central regulators of cell function, including some of the most central processes, such as cell proliferation and intracellular transport (Chi et al., 2013; B. Zhang et al., 2025). In the context of cell migration these signal proteins are thought be master regulators of cell protrusion, cell retraction and associated processes. The primary function of small GTPases is to act as GDP/GTP-regulated molecular switches (Figure 3). They are activated by guanine nucleotide exchange factors (GEFs), which can exchange the nucleotide to GTP, and inactivated by GTPase activating proteins (GAPs), which stimulate the hydrolysis of the bound GTP to GDP. In their active guanosine triphosphate (GTP)-bound form, small GTPases interact with specific molecules, the so-called effector proteins, which

transduce their signals into cellular processes. In their inactive guanosine diphosphate (GDP)-bound form, most small GTPases are considered to be inactive. Small GTPases of the Ras/Rap and of the Rho families are particularly important for cell migration. Members of these two subfamilies are typically associated with the plasma membrane in their active state and are typically stabilized in the cytosol by a solubilization factor in their inactive state.

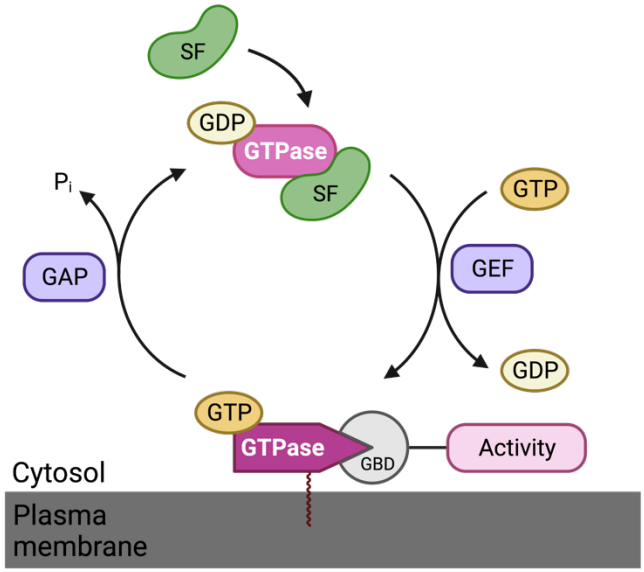

Figure 3: Schematic for the activity cycle of typical GTPases of the Ras/Rap and Rho families: The GTPase can exist in an active, GTP-bound, or an inactive, GDP-bound state. GEFs and GAPs catalyze the switch between these two states. In the active state, the GTPase binds to an effector via a GTPase binding domain (GBD). The active form of Ras/Rap and Rho GTPases preferentially binds to the plasma membrane, while the inactive form is bound to a solubilizing factor (SF) in the cytosol.

Ras subfamily proteins are well-studied oncogenes that are frequently mutated in human cancers. They are critically involved in various cellular processes, especially in proliferation and survival, by mediating growth-factor signaling. Their central role in this major signal transduction system links Ras to many downstream processes that are related to cell migration (Drosten et al., 2010; Soriano et al., 2021), however, their direct, specific role in cell migration is less clear.

Rap GTPases are very closely related to Ras GTPases and share with them many regulators and effectors. They are well known for their role to stimulate both cadherin-based cell-cell-junctions and integrin-based cell-matrix adhesions. In particular, the Rap1a isoform is known to be a central regulator of ´inside-out´ integrin activation via its downstream effector Rap1-GTP-interacting adapter molecule (RIAM) (Guo et al., 2016; Lagarrigue et al., 2016; Miao et al., 2019; Zhang et al., 2017). The related Rap2 isoforms have been studied significantly less but were also linked to integrin functions. However, although they are closely related to Rap1 in structure, Rap2 has also been reported to exert antagonistic functions to Rap1 in controlling endothelial barrier resistance (Pannekoek et al., 2013).

The Rho family GTPase Rac1 is thought to be the master regulator for the formation of flat lamellipodia cell protrusions, by locally activating the multi-protein WAVE regulatory complex (WRC). This complex activates the actin nucleator Arp2/3, thereby promoting actin network branching and growth as introduced in section 1.3.1 and Figure 1 (B. Chen et al., 2017; Nanda et al., 2023).

RhoA, the founding member of the Rho subfamily, is thought to be the master regulator of cell contraction. This is mediated by several effectors, which stimulate actin polymerization, actin-membrane interactions via ERM (ezrin-radixin-moesin) proteins and activate non-muscle myosin. One of the most important Rho effectors is the Rho kinase ROCK, which in turn phosphorylates and activates regulatory subunits of non-muscle myosin. Increased myosin activity then leads to contraction of actomyosin structures and cell retraction (Nanda et al., 2023).

1.4.3 Crosstalk of regulators

To efficiently coordinate downstream processes of protrusion, adhesion and retraction in space and time, tight crosstalk of the associated regulators is needed.

Previous work already suggested crosstalk between Rho and Ras family members that is relevant for cell migration. In particular, Ras/Rap proteins were suggested to act upstream to activate Rac1 (Arthur et al., 2004; Lambert et al., 2002), and also to act downstream of Rac1 (Diekmann et al., 1994; Ferro et al., 2014; Joshi et al., 2023). Rac1 can also stimulate Rho GTPase activity, which in turn was shown to inactivate Rac, tightly coordinating cell protrusion and retraction and enabling protrusion-retraction-cycles (Nanda et al., 2023). Activation of RhoA can also be promoted by Rap1 via talin, implicating further complexity of these signaling networks (Rothenberg et al., 2023). However, while these studies indicate potential crosstalk, the associated kinetics and spatio-temporal correlation of these processes are poorly understood.

1.5 Methods to study cell morphodynamic signal networks

1.5.1 Monitoring the activity state of signal molecules via total internal reflection fluorescence microscopy

To study the activity state of endogenous Rho or Ras/Rap type small GTPases in living, adherent cells, translocation sensors are a highly effective tool (Figure 4). These sensors are fully genetically encoded and based on GTPase binding domains (GBD) of effector proteins for the GTPase of interest, which are fused to a fluorescent protein. To improve their sensitivity via increased avidity, tandem or triple domain repeats can be used. Additionally, the reduction of the expression level of the sensor, for example by using a weak promotor, can be used to prevent competition of the sensor with endogenous effectors. As the active form of Rho or Ras/Rap type GTPases is located at the plasma membrane, these sensors will be recruited from the cytosol to plasma membrane sites with increased amounts of active GTPase. Sensor translocation can then be measured by total internal reflection fluorescence microscopy (TIRF-M). Various GTPase sensors have already been established by using their corresponding, well-characterized GBDs, e.g. a Rac sensor with a triple repeat of the p67^{phox}-GBD (Nanda et al., 2023).

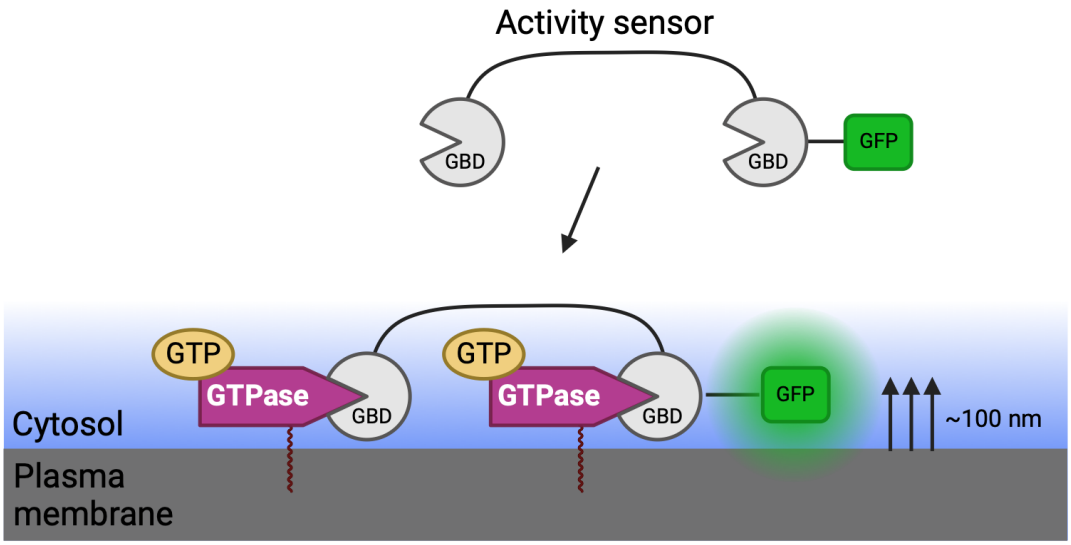

Figure 4: Generic approach to measure the activity state of endogenous small GTPases in living cells. In their active, GTP-bound state, small GTPases of the Rho and Ras family are preferentially localized at the plasma membrane, where they interact with effectors via GTPase binding domains (GBDs). The activity state of these molecules can be monitored by measuring the plasma membrane translocation of a sensor construct that contains a specific GBD fused to a fluorescent protein via total internal reflection fluorescence microscopy (TIRF-M). Sensors that contain tandem repeats of GBDs are more sensitive and can thereby detect even small changes in the local GTPase activity state.

1.5.2 Rapid perturbations in signal networks via optogenetics

To directly investigate highly dynamic interactions and causalities between components of a signal network, rapid, short-term perturbations by optogenetic methods are a very powerful tool. By combining precise spatio-temporal perturbations with measurements of the network response readout via activity sensor constructs, activity crosstalk can be visualized directly.

Several methods were developed to introduce rapid perturbations into signal networks (Kamps & Dehmelt, 2017; Nalbant et al., 2023). One particularly effective method is based on the photoactivatable Rac1 (PA-Rac1) construct, in which a dominant positive Rac1 mutant is fused to the light oxygen voltage (LOV) domain. In the dark, this domain sterically blocks the access to the GTPases effector binding domain. Upon wavelength-specific light activation, a reversible conformational change allows the interaction and activation of effector proteins and downstream processes. Thereby, this construct enabled light-control of local cell protrusion, directly guiding cell migration with light. In combination with translocation sensors, this tool enables direct investigations of potential activity crosstalk downstream of Rac1 (Figure 5) (Nanda et al., 2023; Wu et al., 2009).

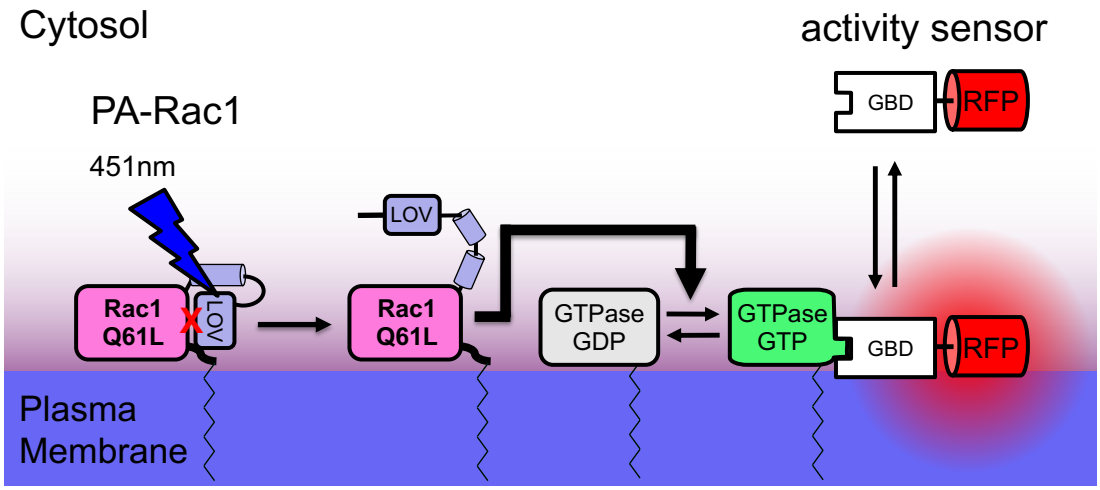

Figure 5: Schematic for light-controlled PA-Rac1 mediated perturbation and its combination with activity measurements in living cells. The photoactivatable Rac1 construct consists of a dominant positive Rac1 mutant fused with the LOV domain, which sterically blocks interactions with effectors. Upon illumination at 451 nm, a reversible change in the LOV domain conformation releases this block and enables activation of effector proteins and downstream processes. Combining this perturbation with activity sensor measurements allows direct investigations of potential activity crosstalk downstream of Rac1.

Another optogenetic method that is suitable for perturbations of Ras/Rap and Rho family GTPases is molecular activity painting (MAP). In this method, a plasma membrane bound HaloTag binds covalently to a photo-uncageable dimerizer. Upon a single light pulse, the chemical dimerizer is locally uncaged. This allows the interaction with a cytosolic eDHFR domain fused to a dominant positive small GTPase, which is lacking the CAAX-box based plasma membrane anchor. This interaction then leads to the plasma membrane recruitment of this dominant positive small GTPase, increasing its local concentration, where it then can stimulate downstream effectors and processes. Again, by combining this method with translocation sensors, potential crosstalk can be visualized directly at the perturbation site (Figure 6) (X. Chen et al., 2017). In a variant of this method, which is called cell attachment MAP or short CA-MAP, the dimerizer can also be uncaged in the whole cell attachment area, for example via a single TIRF illumination pulse.

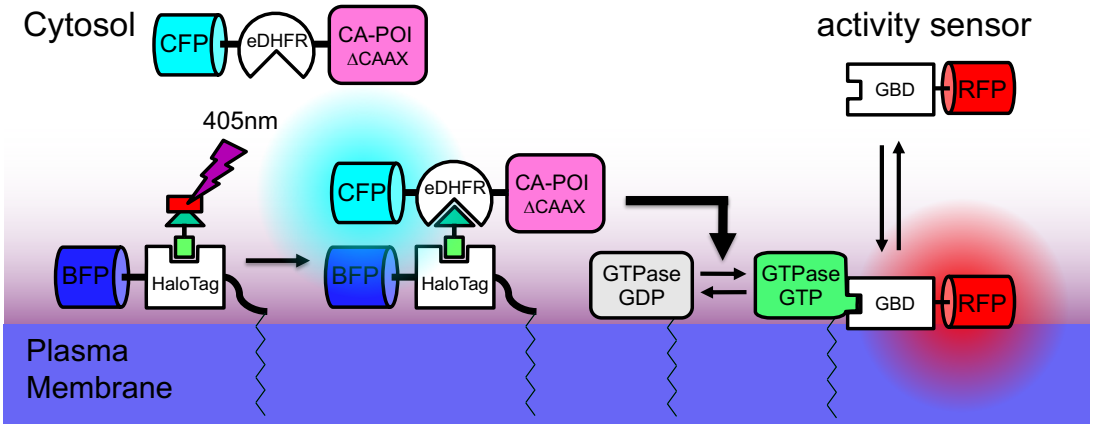

Figure 6: Schematic for the photochemically-induced dimerization method “Molecular Activity Painting” (MAP) and its combination with activity measurements in living cells. A plasma membrane bound HaloTag binds covalently to a photo-caged small molecule dimerizer. Upon illumination with a single, local 405 nm light pulse, the chemical dimerizer can be uncaged, allowing interaction with a co-transfected cytosolic eDHFR domain fused to a dominant positive small GTPase mutant that is lacking its CAAX-motif based membrane anchor. Plasma membrane recruitment of this GTPase mutant increases its local concentration, allowing stimulation of downstream effectors. Combination with translocation sensors allows visualization of potential crosstalk directly at the local perturbation site. In the cell attachment MAP (CA-MAP) variant, the dimerizer is uncaged in the whole cell attachment area via a single TIRF illumination pulse.

2 Objectives

Previous studies described the fundamental importance of Rac and Rap GTPases in the central cellular processes of cell migration and adhesion. In this work, the role and crosstalk between individual Ras and Rap family proteins was investigated in migrating A431 cells. To achieve this, highly sensitive effector-domain based activity sensors and acute optogenetic manipulations were applied. These investigations were combined with knockdown studies to investigate their potential function in cell adhesion and migration. Thereby, these studies are expected to offer deeper insights into the mechanisms of Ras and Rap family protein crosstalk, and how this relates to cell migration.

3 Results

3.1 Spatio-temporal coordination of Rac, Ras and Rap activity in cell migration

3.1.1 Ras/ Rap activity in migrating cells

A431 cells are a keratinocyte derived cell line, which is well-studied in the context of cell migration. Nanda et al. recently found that the cell protrusion stimulating GTPase Rac can activate the cell contraction stimulating GTPase Rho, and that this crosstalk can enhance dynamic protrusion-retraction cycles. These findings raise the question, how signals upstream of Rac regulate its activity in space and time to initiate these cycles. Studies in *Dictyostelium* proposed that Ras/Rap GTPase family members can act upstream of Rac1, but information about these players in mammalian cells remains limited (Plak et al., 2013).

Following an analogous strategy to Nanda et al., new activity sensors for Rap and Ras were generated by fusing tandem copies of the Rap-family effector domain RalGDS-GBD and the Ras subfamily effector domain Raf-GBD to fluorescent proteins (see Figure 4) (Nanda, 2023; Nanda et al., 2023).[1] These sensors preferentially bind the Rap and Ras GTPases in their active, GTP-bound conformation, to allow sensitive detection of their spatio-temporal activity patterns. By ensuring very low expression of these sensors via the very weak delCMV promoter (Watanabe & Mitchison, 2002), competition with endogenous effector proteins can be minimized and the translocation of the sensors from the cytosol to the plasma membrane can be efficiently monitored using TIRF microscopy (Graessl et al., 2017; Nanda et al., 2023).

Ras activity has been previously investigated in many studies via the GBD of the well-characterized Ras effector Raf (Chiu et al., 2002; Weeks et al., 2024). To detect active Rap, the GBD of RalGDS was chosen, as this effector preferentially binds Rap1a compared to Ras (Raaijmakers & Bos, 2009; Shah et al., 2018). However, RalGDS-GBD based translocation sensors are less common and the newly generated 2xRalGDS-GBD sensor therefore required a detailed validation prior to its experimental application.

[1] These sensors were constructed by the PhD candidate Suchet Nanda in the Lab of Leif Dehmelt at the TU Dortmund.

For this validation, the molecular activity painting (MAP) method was used to introduce local Rap perturbations at the plasma membrane, which were combined with parallel sensor response readouts (Figure 6 and 7, X. Chen et al., 2017). Among the five known isoforms of human Rap, Rap1a was used to introduce the local activity perturbations, as this isoform has been studied most extensively and has the highest expression level in A431 cells (Klijn et al., 2014). To generate the perturbation constructs, the CAAX-Box was first deleted from the Rap1a sequence to prevent its targeting to the plasma membrane via endogenous cellular mechanisms. This preferentially cytosolic Rap1a mutant was then fused to the eDHFR (e. coli dihydrofolate reductase) heterodimerization domain. The Halo-Tag was co-expressed as the second heterodimerization domain, which was fused to a CAAX-box to localize it to the plasma membrane (Figure 7). The photocaged dimerizer NvocTMP-Cl forms a covalent bond with to the Halo-Tag to enable controlled plasma membrane targeting of the Rap1a mutant upon local photouncaging within a diffraction limited spot. Additional mutations were then introduced into the Rap1a part of this perturbation construct to control its activity state.

Plasma membrane targeting of dominant positive Rap1a (Rap1a G12V) lead to fast and efficient co-targeting of the Rap activity sensor (Figure 7a), showing that this sensor can indeed interact with active Rap1a in cells. As a negative control, the same perturbation was combined with a control sensor, that lacked the RalGDS-GBD (Figure 7d). As expected, no recruitment of the control sensor was detected. Furthermore, the dominant negative Rap1a S17N mutant was also not able to co-target the Rap sensor to the plasma membrane (Figure 7c), showing that the interaction of the sensor with Rap1a is dependent on its activity state. The wild type Rap1a perturbation showed efficient sensor response, however this was slightly slower compared to the dominant positive Rap1a G12V mutant (Figure 7b). This slower response suggests that the plasma membrane targeted Rap1a wildtype first has to be activated by endogenous plasma-membrane bound Rap GEFs, which then subsequently enable binding of the Rap sensor to active Rap1a.

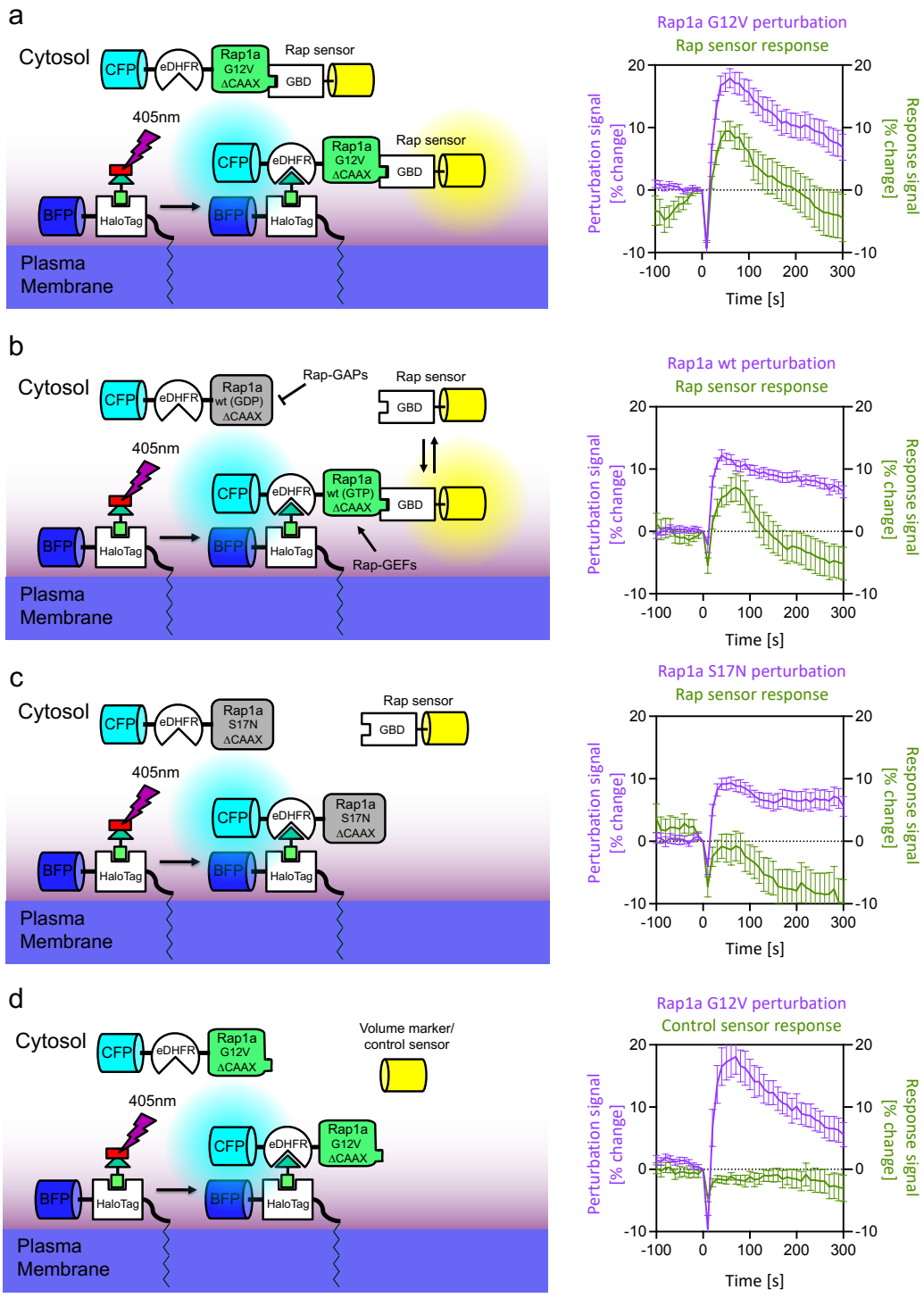

Figure 7: Validation of the newly generated Rap activity sensor mCitrine-2xRalGDS-GBD in A431 cells using the Molecular Activity Painting (MAP) method. (a-d) Schemes for the perturbation and activity response combinations (left) and quantification of dynamic perturbation and sensor response readouts at the perturbation spot (right). a) Validation: combination of Rap1a G12V perturbation with the Rap activity sensor, b) combination of Rap1a (wt) perturbation with the Rap activity sensor, c) negative control: combination of Rap1a S17N perturbation with the Rap activity sensor and d) negative control: combination of Rap1a G12V perturbation with a control sensor lacking the effector domain, (n > 18 cells, 3 indep. experiments). Error bars represent the standard error of the mean (SEM). Figure adapted from Lüttig et al. (2025).

In initial experiments, the Rap and Ras sensors were co-transfected into A431 cells to compare their relative signals. These experiments showed that active Ras is not strongly enriched in subcellular regions of the plasma membrane, bit instead was rather homogenously distributed (Figure 8a-c). The absence of specific localization patterns fits to the well-studied role of Ras type GTPases in cell growth and proliferation. In contrast, the Rap sensor revealed highly dynamic activity patterns even in sessile A431 cells (>40 hours after reseeding) (Figure 8a-c). In particular, transient but substantial activity pulses were observed in central cell attachment areas (Figure 8b, yellow arrows), and sensor signals were also enriched in the small, and very transient cell protrusions that are often generated in sessile cells (Figure 8b, cyan arrows). Highly migratory A431 cells that were freshly reseeded onto fibronectin (<6 hours), showed particularly strong Rap activity close to the protruding cell edge (Figure 8d).

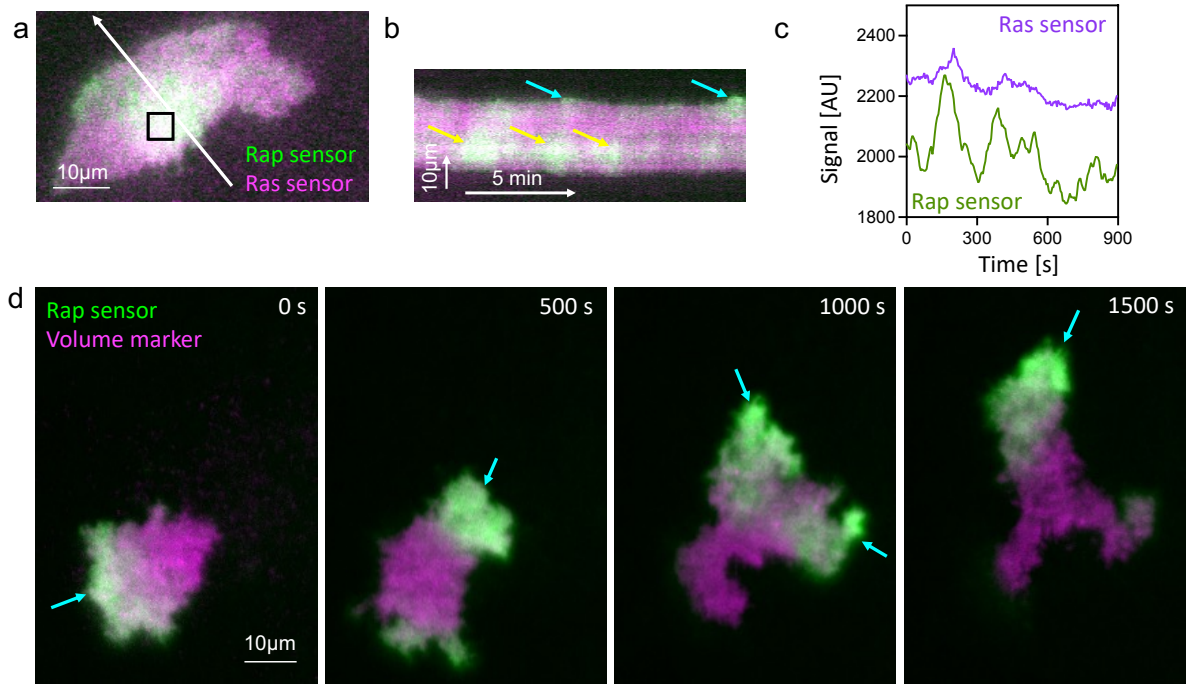

Figure 8: Rap and Ras activity dynamics in A431 cells. a) Representative TIRF image of the Rap activity sensor (mCitrine-2xRalGDS-GBD) co-expressed with the Ras activity sensor (2xRaf-GBD-mCherry) in a sessile A431 cell. b) Kymograph corresponding to the white arrow in a. Yellow arrows point towards the Rap activity pulses in central attachment areas and cyan arrows point to small, transient protrusions. c) Signal intensity changes quantified in the black square in a. d) Sequential timepoints of a migrating A431 cell expressing the Rap activity sensor in combination with a volume marker, imaged with TIRF-M. Cyan arrows point towards the newly formed protrusions. Figure adapted from Lüttig et al. (2025).

To quantitatively analyze the observed activity dynamics of Ras and Rap, a modified version of the ADAPT ImageJ plugin was used for measuring the changes in the GTPase signals in relation to cell edge velocity and in the protrusion and retraction phases (Figure 9) (Barry et al., 2015; Nanda et al., 2023). This analysis revealed that Rap activity correlates tightly and positively with cell edge velocity, with a slight delay of the maximal correlation at 65 seconds after cell protrusion (Figure 9, d, e, m). This was in contrast to active Rac, which correlated very closely with cell edge velocity (Figure 9, j,k,l) (reproduced in Figure 9, j-k; Nanda et al., 2023).

The correlation coefficient for the cell edge velocity is limited by the fact that it cannot distinguish whether the detected activity signal is increasing with a positive velocity during cell protrusion or decreasing with a negative velocity during cell retraction. It also does not indicate the signal intensity with which the sensors are enriched in the cell and instead only quantifies similarity between changes in cell edge velocity and sensor signal changes. An alternative to the cell edge velocity correlation is the direct measurement of signal enrichment during the protrusion or retraction phases. A suitable pipeline for such an analysis was already developed for Nanda et al. and quantifies sensor signal increase at the cell edge in comparison to the whole cell attachment area specifically during the cell protrusion and retraction phases. This protrusion-retraction analyses revealed a very strong enrichment of Rap activity signals (over 80 %), which was maximal at 112 seconds after protrusion, and a substantial reduction (15 %) after cell retraction (Figure 9, f and n). Analogous quantifications for the Ras activity sensor showed much weaker correlation and enrichments compared to Rap activity signals (Figure 9, a-c, g-i, m and n). Nevertheless, the Ras activity signals were still significantly higher compared to signals obtained from a control sensor that was lacking the GBD domain.

Strikingly, there is a clear asymmetry for Rap activity regarding the time ranges before vs. after cell protrusion and retraction, especially for the sensor signal enrichment relative to cell protrusion. Analogous measurements of Rac activity did not show this pattern (reproduced in Figure 9, j-l; Nanda et al., 2023). To quantify this asymmetry, the mean signal enrichment before protrusion was subtracted from the mean signal enrichment after cell protrusion. This quantification confirmed the substantial and significant asymmetry for Rap, and a weak trend was also detected for Ras activity. In contrast, no asymmetry was detected for Rac or the control sensor (Figure 9o).

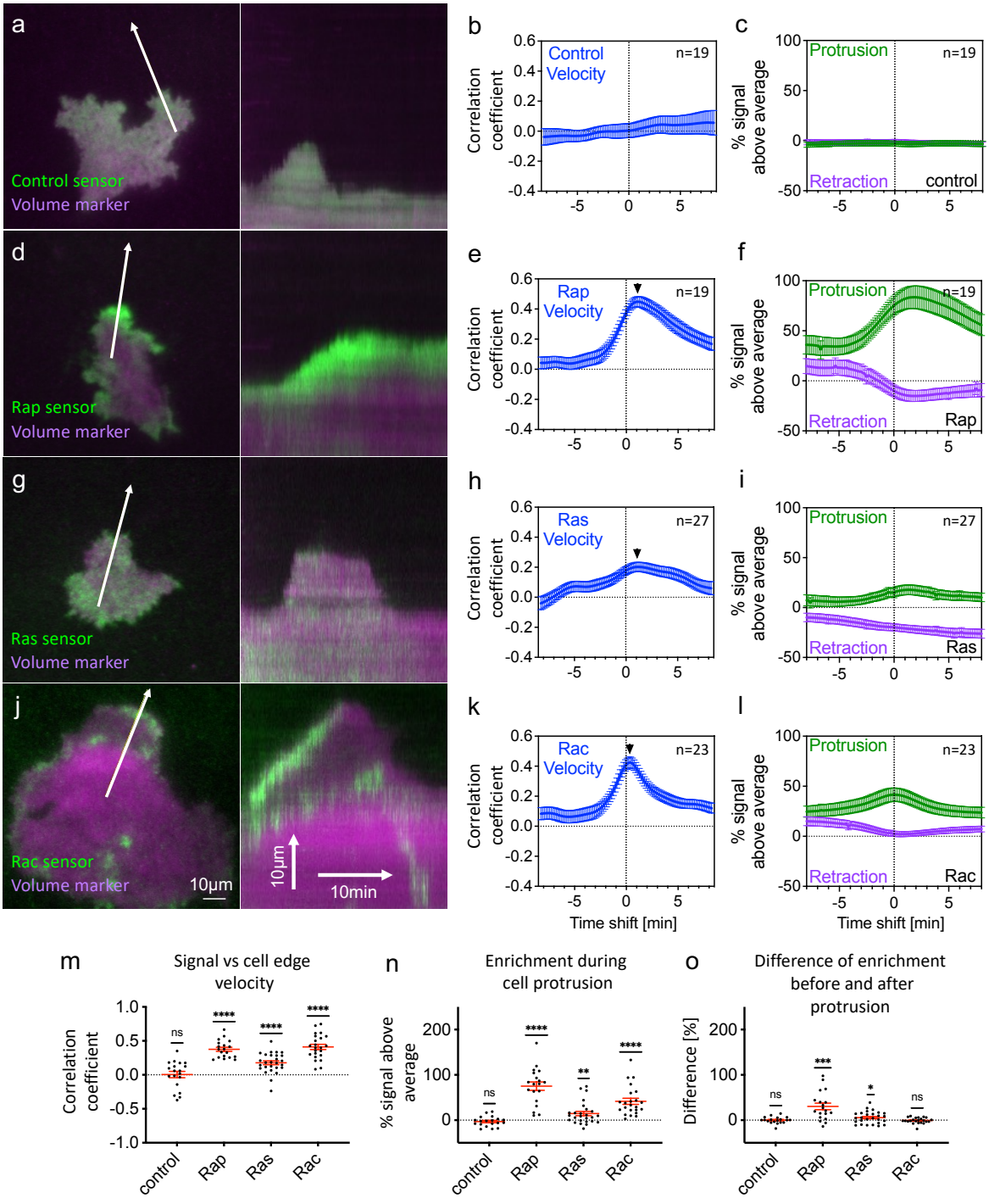

Figure 9: Activity dynamics of Ras and Rap GTPases in migrating A431 cells. a-l) Activity dynamics of the control (a-c), as well as Rap (d-f), Ras (g-i) and Rac (j-l) at the cell periphery of representative, migratory A431 cells during protrusion-retraction cycles. (a, d, g, j) Representative TIRF-M images of the control (a), as well as Rap (d), Ras (g) and Rac (j) activity sensor with a volume marker (left). The kymographs correspond to the white arrows (right). (b, e, h, k) Cross-correlation functions of the activity sensor signals and the corresponding cell edge velocity, plotted against the time shift [min] between these measurements. The black arrow heads point at the time shift with the maximal signal intensity after protrusion. (c, f, i, l) Enrichment of the activity sensor signals in cell protrusions (> 0.5 µm/min) and cell retractions (< -0.5 µm/min), that were normalized to mean control measurements. m) Measurements of the sensor signal vs the cell edge velocity cross-correlation coefficient at a time shift of 0 min from (b,

e, h, k). n) Enrichment measurements of the sensor signal at a time shift of 0 min in (c, f, i, l). o) Difference between the mean sensor signal enrichment before and after cell protrusion (time shift of 0 min) from data shown in (c, f, i, l). Data of Rac activity shown in panels (j-l) and in each last column of (m-o) were reproduced from Nanda et al., 2023 (data is protected by CC BY4.0 license). (*: P<0.05; **: P<0.01; ***: P<0.001; ****: P<0.0001; ns: not significant; one-sample, two-sided t-test; n > 18 cells from at least 3 indep. experiments, exact numbers of cells indicated in panels b, e, h, k and c, f, i, l. Error bars represent the standard error of the mean (SEM)). Figure adapted from Lüttig et al. (2025).

3.1.2 Crosstalk between Rap and Rac GTPases

Rac activity was tightly and closely correlated with cell protrusion, suggesting a strong spatio-temporal link of this regulator with this process. Indeed, it was not possible to detect a shift of the maximal Rac activity enrichment relative to cell protrusion (Δ=0s). Based on the frame interval of 10 seconds used this analysis, the upper limit for the shift of the maximum is therefore smaller than 10 seconds. In contrast, Rap activity was substantially delayed after cell protrusion, with a maximal enrichment at ≈2min after protrusion. Based on this time shift, these results indicate that Rap activity follows Rac activity and thus could support the idea that Rap is activated downstream of Rac.

Simultaneous imaging of the Rap and Rac activity sensors shows both GTPases to be highly active during cell protrusion; however, only Rap activity remained elevated for a prolonged period of time after cell protrusion, while Rac activity quickly declined (Figure 10a). However, small pulses of Rap activity were also observed before initial cell protrusion and before Rac activity was detectable (Figure 10a). Thus, considering an individual cell protrusion event, active Rap was detected before, during and after active Rac, raising the question of how these molecules might be causally related to each other, and if Rap acts upstream or downstream of Rac, or both.

Previous studies provided possible explanations both for a potential crosstalk from Rac to Rap (Lambert et al., 2002; Stefanini et al., 2011), and also from Rap to Rac (Diekmann et al., 1994; Ferro et al., 2014; Joshi et al., 2023). To investigate these potential links, rapid optogenetic activity perturbations were combined with response readout of the signal network.

To test whether Rap indeed can activate Rac, (CA-)MAP experiments were performed. Here, rapid perturbations using the dominant positive Rap1a G12V mutant (see Figure 7a) were combined with the Rac activity sensor as a response readout (see Figure 9, j-l, Figure 10b). In these CA-MAP experiments, perturbations were introduced

selectively in the cell attachment area with a single pulse of 405 nm using the TIRF illumination mode. This generated relatively stable Rap1a G12V perturbations that lasted for more than 5 minutes. Cells responded to this perturbation by a very rapid, short-lived Rac activity response, that again reached baseline levels after around 1.5 minutes (Figure 10, c-e).

This dynamic response suggests a rapid and highly efficient inhibition of Rac upon its activation, which could either be mediated by negative feedback regulation or by a constant inhibition. Interestingly, the Rap/Rac crosstalk was detected both specifically in peripheral cell regions, and also in the entire cell attachment area (Figure 10, e and f). Rac GTPase is well known for its important role in stimulating cell protrusions (Nanda et al., 2023), and indeed, a substantial increase in cell attachment area was observed after the Rap1a G12V perturbation. However, this process was significantly slower compared to the initial activity response, which was expected due to the more complex multi-step mechanism that is underlying this morphological change in cell phenotype (Figure 10, c-g). Interestingly, the Rap/Rac crosstalk was also prominently observed in central cell attachment areas. This suggests that this crosstalk is independent of the observed cell shape changes, which only occurred in peripheral cell regions that were associated with cell protrusion.

This crosstalk within the central cell attachment areas was specifically confirmed using conventional MAP experiments, in which highly local Rap1a G12V perturbations were specifically introduced in diffraction limited spots in the cell center (Figure 10, h-j). Again, a rapid and transient Rac activity response was detected, clearly confirming that in A431 cells, Rap1a acts upstream of the Rac GTPase.

To investigate whether a reciprocal crosstalk from Rac to Rap also exists in these cells, Rac1 perturbations were combined with the Rap activity sensor as a readout (see Figure 9, d-f and Figure 10b). Here, photoactivatable Rac1 (PA-Rac1) was used, which was previously established as an effective method to rapidly stimulate Rac1 activity in living cells (Wu et al., 2009). Combining this tool with continuous TIRF illumination at 445 nm enables the rapid and reversible activation of the Rac1 GTPase in the whole cell attachment area. This Rac1 activation is expected to stimulate the formation of new lamellipodial cell protrusions, and these structures were indeed observed (Figure 10k). In A431 cells, spontaneously generated lamellipodia are typically characterized

by a strong enrichment of Rap activity (Figure 8d and 9d). However, the Pa-Rac1 stimulated lamellipodia did not show an increase in active Rap (Figure 10k). Indeed, no enrichment of Rap activity was observed, neither in the cell periphery, nor in central cell attachment areas. Instead, Rap activity even decreased slightly over the course of 5 minutes (Figure 10, l and m).

These studies revealed a unidirectional activity crosstalk from Rap to Rac GTPases in A431 cells (Figure 10n). Rac is efficiently activated by Rap within seconds and is then inhibited by either negative feedback or a constant inhibition within the next 1.5 minutes (Figure 10, e and i). No strong reciprocal causality could be detected, suggesting that Rap activity is not affected by Rac activity (Figure 10, l and m).

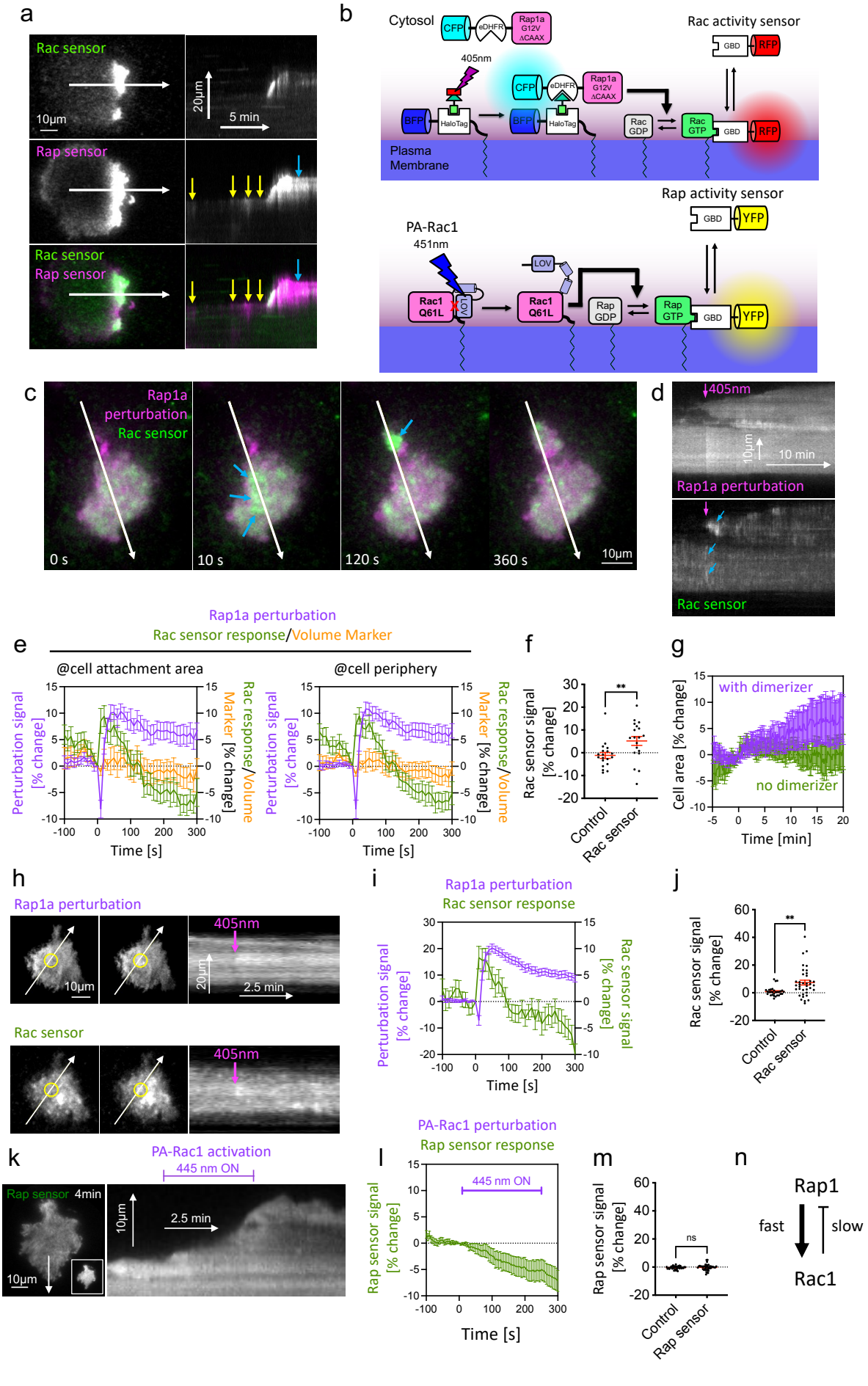
a
Rac sensor
Rap sensor
Rac sensor
Rap sensor
10µm
20µm
5 min
b
Cytosol
CFP
eDHFR
Rap1a G12V ΔCAAX
405nm
BFP
HaloTag
Rac GDP
Rac GTP
GBD
RFP
Plasma Membrane
Rac activity sensor
Rap activity sensor
PA-Rac1
451nm
LOV
Rac1 Q61L
Rap GDP
Rap GTP
YFP
c
Rap1a perturbation
Rac sensor
0 s
10 s
120 s
360 s
10µm
d
405nm
10µm
10 min
Rap1a perturbation
Rac sensor
e
Rap1a perturbation
Rac sensor response/Volume Marker
@cell attachment area
@cell periphery
Perturbation signal [% change]
Rac response/Volume Marker [% change]
Time [s]
f
Rac sensor signal [% change]
**
Control
Rac sensor
g
with dimerizer
no dimerizer
Cell area [% change]
Time [min]
h
Rap1a perturbation
405nm
10µm
20µm
2.5 min
Rac sensor
405nm
i
Rap1a perturbation
Rac sensor response
Perturbation signal [% change]
Rac sensor signal [% change]
Time [s]
j
Rac sensor signal [% change]
**
Control
Rac sensor
k
PA-Rac1 activation
445 nm ON
Rap sensor 4min
10µm
10µm
2.5 min
l
PA-Rac1 perturbation
Rap sensor response
445 nm ON
Rap sensor signal [% change]
Time [s]
m
Rap sensor signal [% change]
ns
Control
Rap sensor
n
Rap1
fast
slow
Rac1

Figure 10: Direct investigations into activity crosstalk reveal unidirectional activation of Rac by Rap. a) Representative TIRF images of a migrating A431 cell that co-expresses the Rap and Rac activity sensors (left) and kymographs corresponding to the white arrows (right). Yellow arrows point to transient Rap activity signals before Rac activation and blue arrows point to prolonged activity of Rap after cell protrusion.[2] b) Scheme for rapid perturbations based on the (CA-)MAP method (top, compare Figure 6) and the PA-Rac1 construct (bottom, compare Figure 5), combined with GTPase activity measurements to measure crosstalk between Rap and Rac. c)-g): Direct investigation of Rap/Rac crosstalk via the CA-MAP method. c) Sequential TIRF-M images of a representative A431 cell co-expressing the constructs mTurquoise2-NES-eDHFR-Rap1a G12V (Rap1a perturbation), mCherry-3xp67phoxGBD (Rac activity sensor) and mTagBFP-Halotag-CAAX (volume marker, not shown); and delCMV-mCitrine (volume marker, not shown)). Images depict time points immediately before and after photouncaging of the photoactivatable dimerizer at the entire cell attachment area with a single TIRF illumination pulse at 405nm. d) Kymographs corresponding to the white arrows in c. Magenta arrows point to the timepoint of perturbation. Blue arrows in c) and d) point to transient Rac1 activity. e) Measurement of Rap1a G12V perturbations at the entire cell attachment area (left) and at the cell periphery (right), combined with quantifications of Rac activity sensor and volume marker signals. f) Measurements of early Rac response at the cell periphery. g) Quantification of the cell attachment area before, during and after photouncaging in the entire attachment area. h)-j): Direct investigation of Rap/Rac crosstalk via the MAP method. h) TIRF-M images of a representative A431 cell co-expressing the same constructs as in c)-g) (left) and the kymographs corresponding to the white arrows (right). i) Measurement of local Rap1a perturbation at a diffraction limited spot combined with quantifications of Rac activity sensor signals corresponding to white circles in h). j) Measurement of early Rac response at the local Rap1a G12V perturbation spot. k)-m): Direct investigation of Rac/Rap crosstalk via photoactivatable Rac (PA-Rac). k) TIRF-M image of a representative A431 cell co-expressing mCerulean-PA-Rac1 (Rac1 perturbation) and mCitrine-2xRalGDS-GBD (Rap activity sensor) (left) and the kymograph corresponding to the white arrow (right). The distribution of mCerulean-PA-Rac1 was acquired at the end of the experimental imaging sequence and is shown in the inset of the left panel. Photoactivation was performed in the entire cell attachment area with TIRF illumination at 445nm. l) Measurement of Rac1 perturbation combined with Rap activity sensor signals in the entire cell attachment area. m) Measurement of the early Rap response in the entire attachment area. n) Proposed unidirectional causality of Rap and Rac in A431 cells based on the GTPase crosstalk investigations shown above. (**: $P<0.01$; ns: not significant; two-sided t-test; (c-g): control: n = 16 cells, experimental condition: n = 19 cells, 3 indep. experiments; (h-j): control: n = 29 cells, experimental condition: n = 37 cells, 3 independent experiments; (k-m): control: n = 38 cells, experimental condition: n = 42 cells, 3 indep. experiments). (f, j, m) Quantifications consider the average intensity signals in the time ranges before (-50s to 0s) and after illumination (0s to 50s). Error bars represent the standard error of the mean (SEM). Figure adapted from Lüttig et al. (2025).

[2] These microscopy-based timelapse recordings were obtained by the PhD candidate Haritha T. Chandran in the Lab of Leif Dehmelt at the TU Dortmund.

3.1.3 Efficient cell attachment is dependent on the Rap1a isoform

Previous experiments showed strong simultaneous activation of Rap and Rac during active cell protrusion of A431 cells (Figure 10a). Further investigations also revealed a more complex spatio-temporal pattern, in which Rap was active for a prolonged period of time after the initial cell protrusion event (Figure 10a; Figure 9 d, f, o). Rap1 is known for its role in stimulating the formation of new cell adhesions. Typically, new adhesions are generated during and after cell protrusion (Boettner & Van Aelst, 2009). We therefore hypothesized that the prolonged Rap activity might play a role in establishing new cell adhesions after cell protrusion.

To test this hypothesis, knockdown experiments were combined with phenotypic readouts of cell adhesion. As Rap1a is highest expressed among the Rap1 subfamily, siRNAs effectively reducing Rap1a mRNA levels of this isoform were identified in a first step (Klijn et al., 2014). The siRNAs “Rap1a siRNA #5” and “Rap1a siRNA #7” showed over 90% mRNA reduction within 48 hours (Figure 11a) and were therefore chosen as two independent reagents to inhibit Rap1a expression in A431 cells. Initial experiments showed that Rap1a depletion via either of the two siRNAs induced a significant reduction in cell adhesion area 96 h after reseeding onto fibronectin coated glass coverslips (Figure 11b and c). This suggests that in A431 cells, Rap1a is necessary for normal spreading, which is a process that it known to require cell adhesion.

Rap1a has also been reported to play a role in integrin-mediated inside-out signaling (Lafuente et al., 2004; Shimonaka et al., 2003). Normal integrin function is of critical importance for the formation and maintenance of focal adhesion structures. Therefore, the effect of Rap1a knockdown on the initial formation of focal adhesions was investigated in subsequent experiments. After replating onto fibronectin, cells were fixed after 3 or 8 hours, stained with Hoechst 33342 dye (nuclei), Phalloidin (actin/ cells) and anti-paxillin antibodies (focal adhesion marker) and investigated via wide-field fluorescence microscopy to quantify focal adhesion formation via CellProfiler (Figure 11d and e).

Especially early after replating, at the 3-hour time point, a role for Rap1a in cell spreading, was confirmed in these experiments by measuring the cell adhesion area. To more directly address focal adhesion formation, the maximal intensity of the paxillin signal and the percentual coverage of the cell adhesion area with focal adhesions was

determined. Both of these measurements showed a strong reduction upon knockdown, confirming the critical importance of Rap1a for normal focal adhesion function in A431 cells in this assay.

These studies provide further insight into the spatio-temporal coordination of Rac and Rap activities in A431 cell migration.

First, based on our direct measurements of Rap and Rac activity patterns in migrating cells, we propose the following sequence of events in the coordination of GTPase activity with protrusion and retraction dynamics in A431 cells (Figure 11f): (1) Rap activity is initially observed already before Rac activity. (2) If Rap activity is sufficiently high, Rac is also activated, initiating a new cell protrusion. (3) During active protrusion, both GTPases are highly active. (4) Subsequently, Rac is downregulated, but Rap activity remains elevated to support subsequent cell adhesion. (5) After a further delay, Rap activity is reduced, which allows subsequent cell retraction and detachment of cell adhesions.

The investigations presented in this chapter further suggest a specific mechanism for the role of Rap1 in cell migration (Figure 11g): (1) The initial small pulses of Rap activity are presumably stimulated by processes that act upstream such as growth factor receptor signaling. (2) Rap1a can then unidirectionally activate Rac in a fast and efficient manner to stimulate cell protrusion. (3) Rac is subsequently also downregulated again during prolonged elevation of Rap activity (Figure 10e and i). This suggests that either negative feedback regulation or a constant inhibition of Rac occurs in A431 cells. One potential mechanism could be the downregulation of Rac by Rho activation (Nanda et al., 2023) and subsequent recruitment of Rac GAP activity (Guilluy et al., 2011). (4) Rap activity remains elevated to support subsequent cell adhesion, thereby stabilizing the newly formed cell protrusion (Figure 11g). This proposed mechanism can explain how A431 cells ensure effective protrusion by using a hierarchical, spatio-temporally coordinated crosstalk from Rap1a to Rac1 to couple a newly formed protrusion to subsequent cell adhesion.

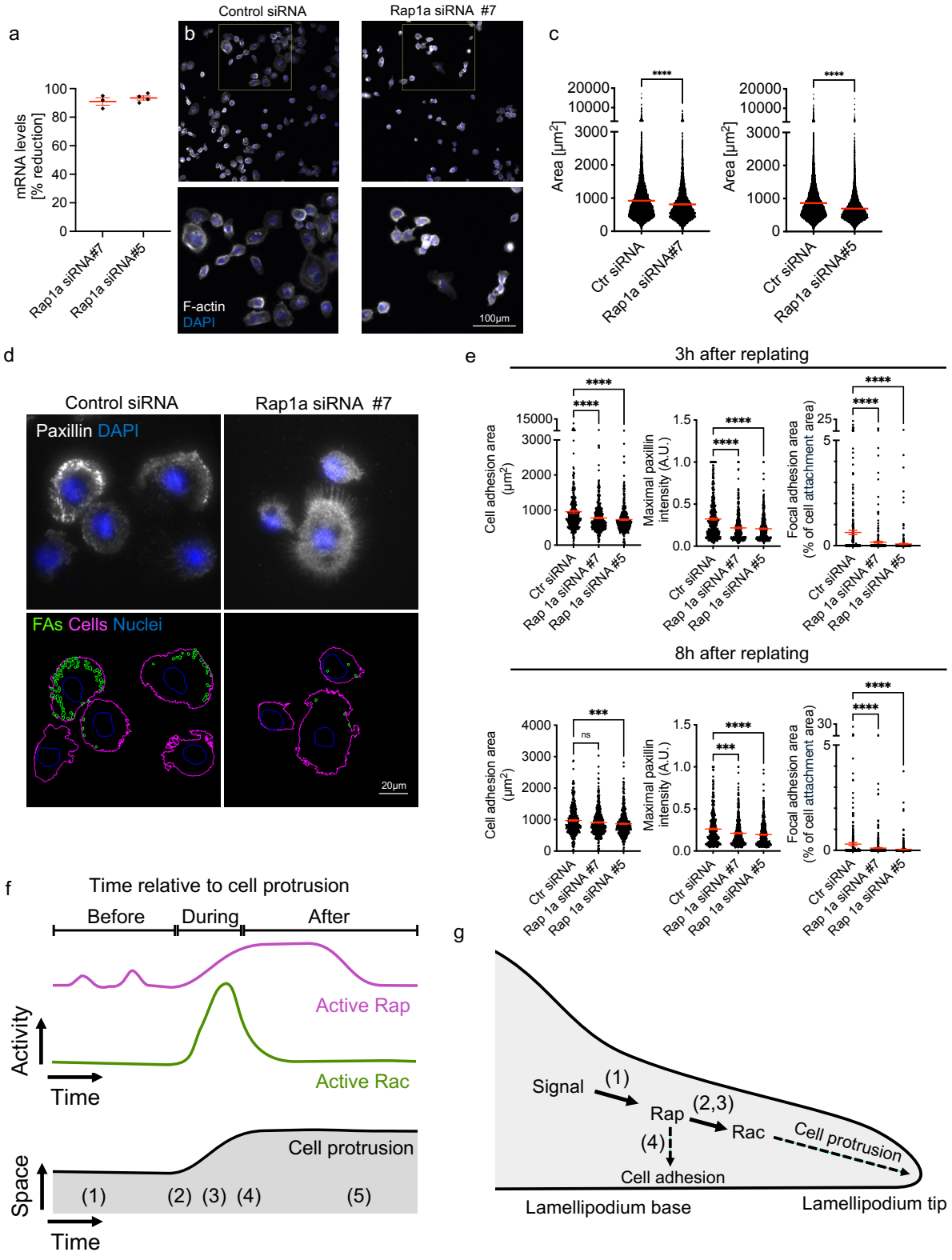

Figure 11: The Rap1a isoform is necessary for efficient cell attachment of A431 cells. a) Quantification of Rap1a siRNA-mediated knockdown after 48 hours; mRNA levels were obtained via qPCR. Rap1a mRNA reduction was highly efficient (siRNA#7: 91±3%, n=3 and siRNA#5: 93.4±1%, n=4; mean±SEM). (b and c) Effect of Rap1a knockdown on the size of the cell attachment area 96 h post knockdown. b) At 8 hours post seeding onto fresh fibronectin, A431 cells were fixed and stained for filamentous actin (Phalloidin) and nuclei (Hoechst 33342). c) Quantification of the cell attachment area was performed

with CellProfiler (left: control: n = 13578 cells, siRNA#7 n = 8539 cells, from 3 independent experiments; right: control: n = 20375 cells, siRNA #5 n = 11920 cells, from 4 independent experiments). (d and e) Effect of Rap1a knockdown on the formation of focal adhesions. d) At 3 hours post replating onto fresh fibronectin, A431 cells were fixed and stained for filamentous actin (Phalloidin), nuclei (Hoechst 33342) and the focal adhesion marker paxillin (mouse anti-Paxillin monoclonal antibody Clone 349). Representative image composites of Paxillin (TIRF-M) and nuclei (wide-field microscopy) (top). Focal adhesions, cell outlines and nuclei objects were identified via CellProfiler and shown as colored outlines (bottom). e) Cell adhesion area, maximal paxillin signal per cell and the fraction of cell adhesion area covered by focal adhesions were quantified 3 and 8 hours after reseeding onto fresh fibronectin 96 h post knockdown (n > 377 cells from 3 independent experiments). f) Schematic depiction of the Rap and Rac activity state related to cell protrusion in space and time. (1) Rap activity is initially observed already before Rac activity. (2) If Rap activity is sufficiently high, Rac is also activated, initiating a new cell protrusion. (3) During active protrusion, both GTPases are highly active. (4) Subsequently, Rac is downregulated, but Rap activity remains elevated to support subsequent cell adhesion. (5) After a further delay, Rap activity is reduced, which allows subsequent cell retraction and detachment of cell adhesions. g) Proposed role of the Rap GTPase in cell protrusion of A431 cells. (1) The initial small pulses of Rap activity are presumably stimulated by processes that act upstream such as growth factor receptor signaling. (2) Rap1a can then unidirectionally activate Rac in a fast and efficient manner to stimulate cell protrusion. (3) Rac is subsequently also downregulated during prolonged elevation of Rap activity. (4) Rap activity remains elevated to support subsequent cell adhesion, thereby stabilizing the newly formed cell protrusion. Error bars represent the standard error of the mean (SEM). (****: $P<0.0001$; ***: $P<0.001$; ns: $P>0.05$; two-sided student's t-test (c) or ordinary one-way ANOVA with Dunnet's post test (e)). Figure adapted from Lüttig et al. (2025).

3.2 Comparative analysis of Rap1 and Rap2 function in cells[3]

3.2.1 Role of Rap1 and Rap2 in cell adhesion and cell migration

As shown in Figure 11 b-c, knockdown of Rap1a lead to a significant reduction in cell adhesion of A431 cells on fibronectin, further supporting the idea that this molecule is able to stimulate cell-matrix adhesion. This raises the question, how other Rap family members might affect this fundamental cellular process. While Rap1a is the highest expressed Rap family member in A431 cells, all five isoforms are detectable in this cell line. Interestingly, previous studies suggested antagonistic cellular functions of Rap1 and Rap2 in the regulation of endothelial barrier function (Pannekoek et al., 2013), a process that involves cell-cell adhesion. While cell-cell and cell-matrix adhesion differ in many molecular aspects, for example concerning the receptors that mediate these processes, some common regulatory components are known (Burute & Thery, 2012). To investigate the role of Rap2 in A431 cells, analogous phenotypic analysis was performed after siRNA-mediated depletion of Rap2b. The isoform Rap2b was chosen as it is the highest expressed Rap2 subfamily member in the A431 cells (Klijn et al., 2014). Quantification of Rap2b siRNA-mediated knockdown after 48 hours showed that the remaining mRNA levels were quite variable depending on the siRNA sequence (reduced by 84.8±6% with siRNA#7, n=3 or by 26±9% with siRNA#6, n=4; mean±SEM, obtained via qPCR). Interestingly, cells treated with highly effective Rap2b siRNA#7 showed a significant increase in cell adhesion area, thus displaying the opposite phenotype to Rap1a knockdown (see Figure 12). However, treatments with the less effective Rap2b siRNA#6 did not confirm this observation and even suggested a slight reduction of the cell adhesion area.

[3] Preliminary results were obtained in my Master´s Thesis in the Lab of Leif Dehmelt at the TU Dortmund (2022). The data that is shown here includes these preliminary results and an additional 4th repeat for the siRNA treatments Rap1a #5 and #7 as well as a 3rd repeat for the siRNA treatments Rap2b #6 and #7. These additional repeats comprise all experiments that are shown, including the determination of knockdown efficiency by qPCR, quantification of cell attachment area (Figure 12), random migration experiments (Figure 13) and were critical to clearly deduce the proposed mechanism (Figure 14).

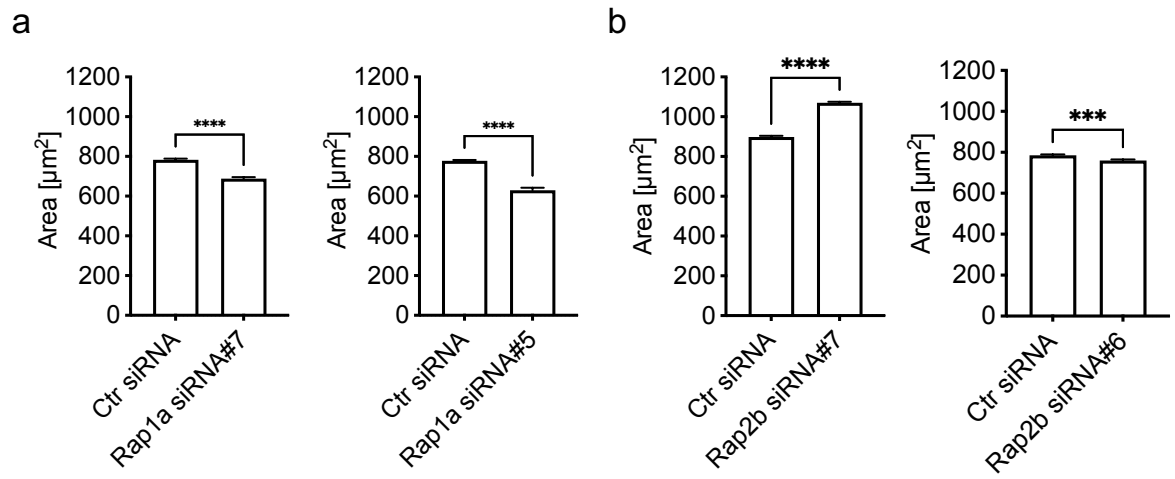

Figure 12: a-b) Quantification of area size was performed with CellProfiler. Contents of a were reproduced from Figure 11c for easier comparison. (****: P<0.0001; ***: P<0.001; two-sided student's t-test; a) left: control: n = 13578 cells, siRNA1a#7 n = 8539 cells, from 3 indep. experiments; right: control: n = 20375 cells, siRNA1a#5 n = 11920 cells, from 4 indep. experiments; b) left: control: n = 15751 cells, siRNA2b#7 n = 17647 cells, from 3 indep. experiments; right: control: n = 16349 cells, siRNA2b#6 n = 13591 cells, from 3 indep. experiments). Quantification of Rap2b siRNA-mediated knockdown after 48 hours; mRNA levels were obtained via qPCR. Rap2b mRNA reduction was efficient (siRNA2b#7: 84.8±6%, n=3 and siRNA2b#6: 26±9%, n=4; mean±SEM). Error bars represent the standard error of the mean (SEM). The column graphs in panel a are identical to those in Figure 11 c and are shown here to enable for comparison with the analogous analyses of the Rap2b knockdown effect.

We next investigated how knockdown of Rap1a or Rap2b affects the migration of A431 cells. In particular, spontaneous non-directional migration was investigated to measure the velocity and directionality of control and knockdown cells. As expected, substantially different migration types could be observed (see Figure 13).

After Rap1a depletion, we found an increase in migration velocity with one of the siRNAs, but no significant effect with the other siRNA. Concerning Rap2b, knockdown with either of the two siRNAs lead to decreased migration velocity. Measurements of migration directionality suggested some general trends but did not reveal significant differences in comparison to the respective controls.

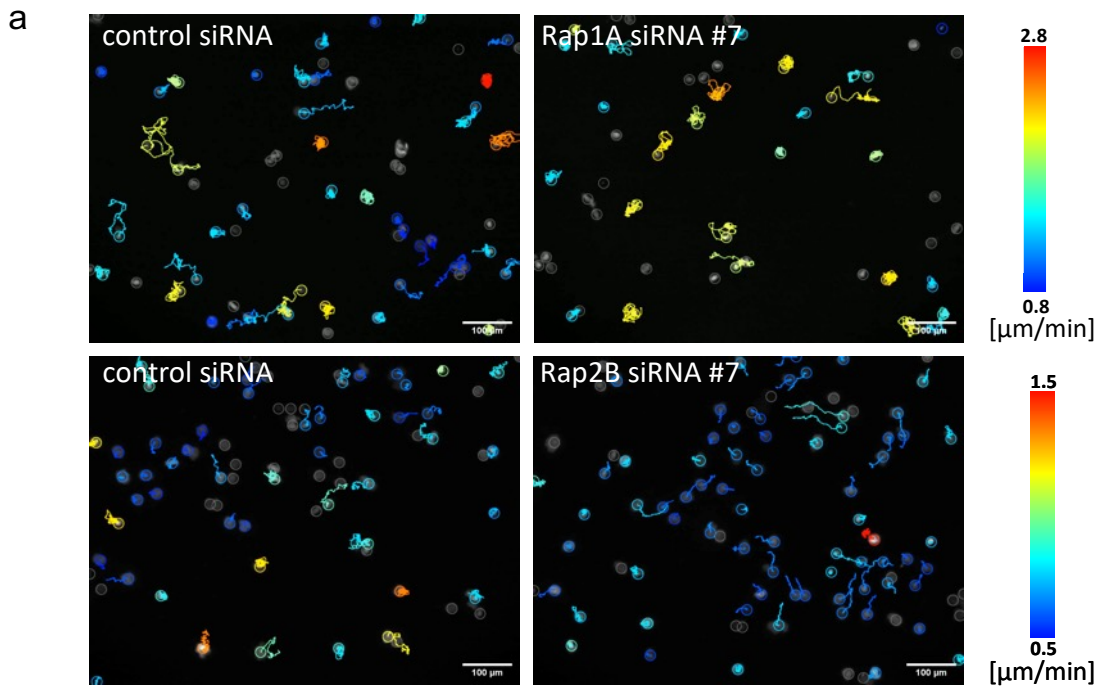

Rap 1A #7: faster, less directional
Rap 2B #7: slower, more directional

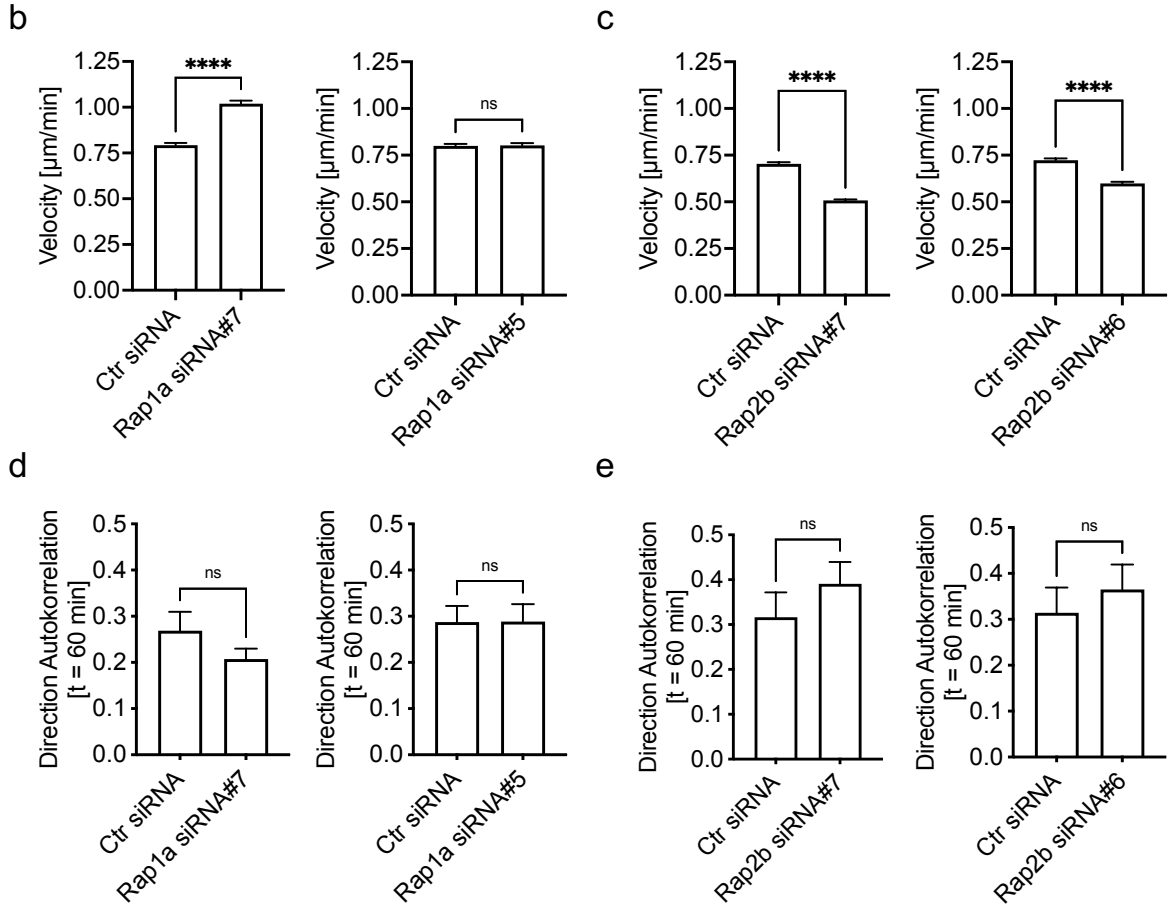

Figure 13: a) Nuclei of Rap1A siRNA#7 and Rap2B siRNA #7 treated A431 cells in comparison to respective control cells. Automated nuclei-tracking was performed using the Fiji Plugin TrackMate. b-c) Quantification of migration velocity performed with the Fiji plugin Chemotaxis (Ibidi GmbH, Martinsried, Germany). (****: P<0.0001; ns: P>0.05; two-sided student's t-test). d-e) Quantification of direction autocorrelation values performed by Excel Macros (Direction Autocorrelation). (ns: P>0.05; two-sided student's t-test). (b+d) left: control: n = 511 cells, siRNA1a#7 n = 403 cells, from 3 indep. experiments; right: control: n = 628 cells, siRNA1a#5 n = 581 cells, from 4 indep. experiments; c+e) left: control: n = 682 cells, siRNA2b#7 n = 729 cells, from 3 indep. experiments; right: control: n = 664 cells, siRNA2b#6 n = 660 cells, from 3 indep. experiments). Error bars represent the standard error of the mean (SEM).

Overall, the investigations of the effect of Rap1a or Rap2b knockdown on cell attachment and migration suggest opposite phenotypes. However, as the effects were not always consistent with the two most effective siRNAs, these observations are still ambiguous to some extent.

While the inhibitory effect of Rap1a knockdown on cell adhesion was clear, the corresponding stimulatory effect of Rap2b knockdown was less clear. One potential explanation could be that the precise dosage of Rap2b might be important for cell adhesion, and that the weaker knockdown was not able to stimulate cell adhesion sufficiently.

Cell migration on the other hand is a more complex process that requires the coordination of several processes, and its link to cell adhesion is not trivial, and both too little and too much adhesion might prevent efficient cell migration (Case & Waterman, 2015). It is thus not surprising that these experiments were associated with some variability concerning the distinct siRNAs.

The observed overall trend towards opposite phenotypes for Rap1a and Rap2b could be explained by differences in their specific effectors (see Figure 14). Previous studies already established that Rap1a can activate talin, which binds and subsequently activates integrins. For Rap2b, no causal chain of links was published so far that links this molecule to cell adhesion, however two separate studies might hint towards a potential mechanism: First, MAP4K4 was identified as a Rap2 subfamily specific effector (Machida et al., 2004), and in a different study, MAP4K4 was shown to inhibit talin-mediated activation of integrins by activation of moesin (Vitorino et al., 2015). Taken together, these two processes could enable negative regulation of cell adhesion by Rap2b (Figure 14).

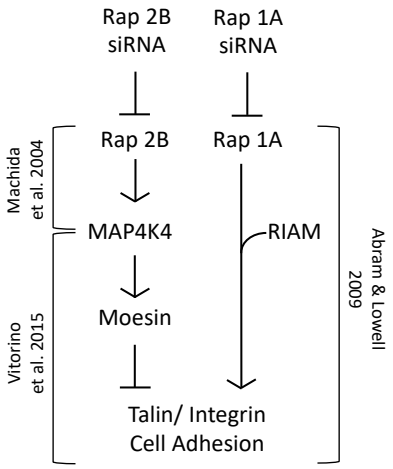

Figure 14: Proposed mechanism for opposite phenotypic effects of Rap1a and Rap2b knockdown on integrin-mediated cell adhesion. While Rap1a was previously described to enable integrin mediated cell adhesion (Abram & Lowell, 2009), no causal chain of links connecting Rap2b to cell adhesion was published. However, MAP4K4 was identified as a Rap2 specific effector protein (Machida et al., 2004) and later, MAP4K4 was shown to inhibit talin-mediated activation of integrins by activating moesin (Vitorino et al., 2015).

4 Discussion

The small GTPases Ras, Rac and Rap are key players in various physiological processes. Ras has been extensively studied for its role in the control of cellular growth and differentiation, while Rac is best known for its role in inducing cellular protrusions. The GTPase Rap is most closely related to Ras, however, its main functions are not thought to be related to cell growth and differentiation but rather related to cell adhesion. While Ras and Rap share more than 50 % sequence identity, differences in interactions with GEFs, GAPs and effectors are thought to enable these functionally distinct roles of Rap1 and Ras (Raaijmakers & Bos, 2009; Scrima et al., 2008).

4.1 Activity patterns of the signal molecules Rap and Rac and their crosstalk in cells

Both cell protrusion and cell adhesion are central processes during cell migration, however, how these processes are coordinated with each other in space and time within individual cells was still poorly understood. To gain a deeper understanding of this coordination, this thesis focused on investigations of signal crosstalk between the cell adhesion regulator Rap and the cell protrusion regulator Rac.

To address this question, highly sensitive, effector-domain based activity sensors were used to measure dynamic activity patterns of Ras, Rac and Rap in migrating A431 cells. These studies confirmed previous observations, that Rac activity correlates tightly with cell protrusion (Nanda et al., 2023), and uncovered that Rap activity largely overlaps with Rac activity, and was additionally also observed before and after maximal cell protrusion. In particular, the tight spatio-temporal coupling of Rap and Rac seen in Figure 10a suggested that the activity of these two small GTPases are linked via crosstalk. To investigate potential causalities that might mediate such crosstalk, rapid optogenetic perturbations were introduced within individual, living cells, and combined with parallel activity readouts. These experiments revealed that Rap1 can activate Rac very quickly and efficiently, while reciprocal crosstalk was undetectable, suggesting an instructive role of Rap in the generation of new cell protrusions. Additionally, Rac was found to be slightly downregulated in the continuous presence of active Rap, suggesting a negative feedback regulation or strong constant inhibition of Rac, for example via activation of the related GTPase RhoA (Nanda et al., 2023).

This newly uncovered, unidirectional hierarchy between Rap and Rac is summarized in Figure 15 in the context of their function to stimulate adhesion and protrusion, together with previously identified signal network crosstalk that coordinates these functions with cell contraction/retraction. The idea that Rap plays a central role in cellular adhesion is further supported by the prolonged presence of active Rap after the actual cell protrusion event and thus might play an important role in stabilizing newly formed cell protrusions.

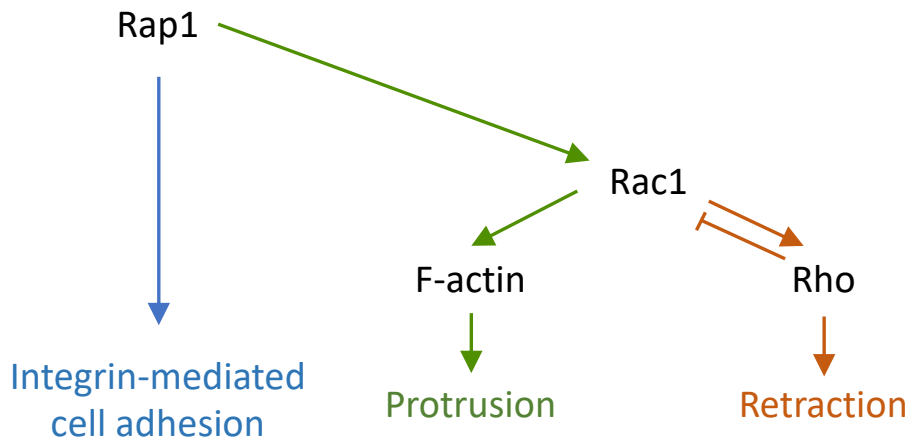

Figure 15: Schematic signal network connecting Rap, Rac and Rho activity in A431 cell migration. Rap1 mediated activation of Rac generates new cell protrusions via F-actin and time-delayed retraction processes via Rho, while stimulating integrin-mediated cell adhesion.

4.2 Functional Role of Rap1 in cell function and disease

Efficient cell migration and homeostasis in healthy tissues is strongly dependent on effective spatio-temporal coupling of cell protrusion to cell adhesion. Loss of initial, tightly regulated adhesion characteristics is a major hallmark of cancer and often associated with malignant transformation and metastasis (Janiszewska et al., 2020). Indeed, previous studies have demonstrated a clear link between Rap1 dysregulation and cancer invasiveness and metastasis (Jaśkiewicz et al., 2018; Y. L. Zhang et al., 2017). The causal links are however quite complex, and constitutive activation of Rap1 has been observed to either support or reduce tumor invasion, suggesting cancer subtype specific effects of increased Rap1 signaling (Looi et al., 2020).

Activation of Rap involves several different steps and can be mediated by a variety of extracellular and intracellular cues, including receptors like growth factor receptors or second messengers such as cAMP (Gloerich & Bos, 2011; Zwartkruis et al., 1998). Apart from Rap1 specific GEFs such as Epac or PDZ-GEF, other important players in

the activation of Rap1 are CalDAG-GEFI, II and III, which also activate Ras (Yamashita et al., 2000). Overlaps in Ras and Rap signaling already intertwine Rap into the commonly known oncogenic pathway of Ras, however, distinct Rap1 signaling is also associated with pathological processes: Enhanced Rap1 activation is linked to several cancer hallmarks including increased cell migration, adhesion and survival, ultimately thought to contribute to cancer metastasis (Bailey et al., 2009).

4.3 Differential cellular functions of Rap1 and Rap2

While Rap1a has been extensively studied both in physiological and in pathophysiological contexts, the roles of other Rap isoforms are less clear, and some previous studies even suggested antagonistic effects between Rap1 and Rap2 subfamily members in cell-cell adhesion (Pannekoek et al., 2013). However, if such an antagonistic relationship also extends to cell-matrix adhesion was not known. In this thesis, siRNA knockdown of Rap1a confirmed an important stimulatory function of this specific isoform in cell-matrix adhesion of A431 cells. Interestingly, subsequent investigations of the Rap2b isoform supported an antagonistic effect compared to Rap1a, thus supporting the idea that these isoforms might indeed also act antagonistically in cell-matrix adhesion (Figure 12 and Figure 13).

The Rap2b knockdown studies were performed with two siRNAs, out of which only one efficiently reduced Rap2b mRNA levels (84.8±6% with siRNA2b#7), while the other showed a much weaker effect (26±9% with siRNA2b#6). Interestingly, the highly effective Rap2b siRNA#7 induced a significant increase in cell adhesion area, thus displaying the opposite phenotype to Rap1a knockdown (see Figure 12). However, treatments with the less effective Rap2b siRNA#6 did not confirm this observation and even resulted in a slight reduction of the cell adhesion area. Given the inefficient knockdown by siRNA#6, it is likely that the lack of a clear phenotype is due to the large residual amount of Rap2b in this condition. Unfortunately, out of the 4 commercially available On-target plus siRNAs, the two remaining reagents were even less efficient in targeting Rap2b, and the role for Rap2b in cell adhesion is therefore currently not fully resolved.

In the random migration experiments, Rap2b knockdown showed a consistent decrease in velocity for both siRNAs, which was opposite to the increase induced by Rap1a siRNA#7. Unfortunately, Rap1a siRNA #5 did not have an effect on migration,

although both siRNA#7 and siRNA #5 highly efficiently knocked down Rap1a. This inconsistency in the cell migration phenotype might be related to the complexity of cell migration and how it is related to cell adhesion. In particular, previous studies showed that an intermediate level of cell adhesion is optimal for cell migration speed, and that both higher and lower adhesion interfere with this process (Gupton & Waterman-Storer, 2006). Due to this complexity, it is difficult to predict, how the manipulation of a mechanism that regulates adhesion, such as Rap1 amounts, affect migration speed, and the observed differences might be due to small differences in the cellular reaction to the two distinct siRNAs. On the other hand, the effects on the much simpler and more direct readout on focal adhesion strength and cell spreading were very clear and consistent for both Rap1a siRNAs. Taken together, while a stimulatory role for Rap1a in cell adhesion is very clear in A431 cells, observations concerning differential effects of Rap1a vs Rap2b give a first hint at their potentially opposite roles, which however will need further verification and orthogonal approaches such as gene knockout or overexpression.

A potential physiological function of an antagonistic link between Rap1 and Rap2 could be the need for a well-balanced regulation of cellular adhesion. Constant remodeling of adhesive structures during active cell migration requires balanced adhesion assembly as well as disassembly, and dysregulation of Rap1 activity was previously shown to be associated with tumor invasion and metastasis (Y. L. Zhang et al., 2017). Therefore, appropriate negative regulation of integrin mediated cell adhesion in space and time, for example by Rap2, is of equal importance to function and migration as properly controlled positive adhesion regulation by Rap1 and thus merits further investigations.

4.4 Requirements for the generation of Rap activity pulses and waves

Apart from the clear enrichment in transient protrusions, near the leading edge of actively migrating cells, Rap activity was also clearly detected in pulsatory patterns in more central cell attachment areas of sessile A431 cells (Figure 8 a-c). Such pulses and propagating waves have been previously observed in another GTPase signal network, in which the small GTPase Rho generates dynamic activity patterns in controlling cell contraction (Graessl et al., 2017). These activity patterns were specifically observed with the Rap sensor, and not seen in A431 cells with the Ras or

control sensors. This clearly shows that these apparent activity patterns are not artifacts that derive from membrane movements, but indeed originate from altered local signaling. Such pulses and propagating waves are often observed in so-called excitable signal networks, which typically include both positive and negative feedback control. Potential mediators for positive feedback might include RapGEFs that act both as Rap activators and as Rap effectors, like PDZ-GEF, PLCε and Epac (Raaijmakers & Bos, 2009). Recent studies in *Dictyostelium* suggested negative feedback between Rap1 and a homologue of MST1/2, a mammalian tumor suppressor, KrsB (Kinase responsive to stress B) (Artemenko et al., 2025). A combination of positive and negative feedback loops could generate the pulsatory Rap activity patterns that we observe in A431 cells (Qiao et al., 2022).

4.5 Relation of Rap activity sensor signals to Rap1 vs Rap2 activity

As the Rap activity sensor can detect both Rap1 and Rap2 activity, it is not possible to differentiate which isoform of Rap is responsible for the observed activity patterns. Furthermore, the observed Rap activity patterns are very complex, and it is therefore possible that Rap1 and Rap2 differentially contribute to qualitatively different types of patterns, such as the enrichment at cell protrusions or the enrichment in transient pulses and waves.

Given the well-established role of Rap1 in stimulating cell adhesion, the requirement for increased adhesion after cell protrusion, and the clearly demonstrated activity crosstalk from Rap1a to Rac shown in this study, the simplest interpretation of the available data is that active Rap1 is the major contributor to the increased activity sensor signals during and shortly after cell protrusion. However, Rap2 could potentially also be active during this process, for example by have a limiting, regulatory function.

While the experimental data and logic concerning Rap isoforms in cell protrusions appears relatively clear, it is more difficult to interpret the role of Rap1 vs Rap2 in the generation of subcellular activity pulses and waves. In particular, as these patterns are not linked to cell shape changes, it is unclear, if these pulses are associated with increased or decreased cell adhesion, and thus could be related either to Rap1, to Rap2, or both. It is for example well-known that focal adhesions in more central cell areas are constantly remodeled and the Rap activity pulses and waves could play a role in this process.

Interestingly, no sensor enrichment was detected in cell retractions, where cell adhesion has to be inhibited. Thus, if Rap2 is indeed a negative regulator of cell adhesion, this does not result in a local enrichment of active Rap2. Instead, Rap2 might act as a global inhibitor with constant activity, which would only be detected as an offset in the signal within cells and would not give rise to distinct local activity sensor enrichments.

4.6 Development of Rap isoform specific activity sensors

The development of either a Rap1 or of a Rap2 specific activity sensor would be very valuable to resolve these unanswered questions. By combining such a sensor with the pan-RAP activity sensor used in this study, the ratio between their signals could be used to yield both Rap1 and Rap2 specific signals.

Several efforts in this direction that were undertaken in this thesis did not result in the generation of a useful Rap2 activity sensor (see 8.1). These efforts focused on the few, known Rap2 effectors, and were based on two distinct domains, the CNH domain of MAP4K4 and the RUN domain of Rufy3. Unfortunately, the application of these domains in cells was difficult, and transfection efficiency and protein expression levels were very low, and furthermore lead to typical stress-related cell phenotypes. This indicates, that the isolated domains might not fold correctly in mammalian cells, or that they might have additional, dominant negative or dominant positive effects. Future approaches could involve other domains reported to solely bind Rap2, like RPIP8, its homologue RPIPx, or TNIK, or a broader range of known effector domains, for which their relative affinity to active Rap1 vs Rap2 is not yet known (Miertzschke et al., 2007). Alternatively, based on existing structural models or Alphafold-based predictions, point-mutations could be introduced into the current RalGDS-based pan-RAP activity sensor with the aim to develop Rap1 or Rap2 specific variants (H. Zhang et al., 2013). For example, it was proposed that Serine 39 in Rap1 and Phenylalanine 39 in Rap2 that engage in effector binding, might enable isoform-specific binding of other effectors, such as MAP4K4 (Miertzschke et al., 2007). The relative binding affinity to Rap1 and Rap2 of sensor candidates could be tested directly in living cells via the MAP system using the Rap1aG12V and Rap2bG12V perturbation constructs generated in this thesis.

4.7 Mechanistic basis for spatio-temporal Rap activity patterns and activity crosstalk

The direct crosstalk analyses in this study clearly revealed a unidirectional crosstalk from Rap1 to Rac family GTPases. Mechanistically, the Rap1-activity dependent Rac activation might be mediated by RacGEFs, which also act as Rap effectors. Vav2 and Tiam1 are two Rac GEFs that might be able to fulfill this role, as they were previously shown to be activated by Rap1 (Arthur et al., 2004). However, several aspects that are related to Rap activity patterns and Rap activity crosstalk remain unclear. In particular, it remains to be investigated, if Rap2 has an effect on Rac, and how Rap activity itself is regulated to generate pulsatile activity patterns.

Future investigations of these mechanisms can build on the combination of rapid Rap1 or Rap2 activity perturbations via the “Molecular Activity Painting” method and readouts based on activity sensors or translocation of intermediate signal molecules, such as GEFs, GAPs or effectors. Such an approach could for example be used to investigate links between active Rap isoforms and RapGEFs like PDZ-GEF, PLCε and Epac, which might be of particular interest, as they could potentially close a positive feedback loop, based on the idea that these RapGEFs are also strong candidates to function as Rap effectors (Raaijmakers & Bos, 2009). Investigations of the interplay between individual Rap isoforms would greatly benefit future studies, as they will be able to resolve ambiguities and thus might reveal clearer signaling network structures. This thesis already supports previous reports of antagonistic effects of the Rap1 and Rap2 subgroups, and earlier studies rarely differentiated between these groups when addressing interactions of Rap proteins with effector proteins, scaffold proteins, GEFs and GAPs. Future experiments could also include expansion of the Rap isoform knockdown studies, by confirming the observed phenotypes with knockout cell lines, performing rescue experiments or utilizing orthogonal approaches such as overexpression to decipher the Rap1 and Rap2 isoform functions in more detail.

In conclusion, this thesis reveals specific spatio-temporal patterns of Rap activity and a unidirectional crosstalk from Rap to Rac, which links the central processes of cell protrusion and cell adhesion. Further investigations into the Rap family suggest an antagonistic relationship between the major Rap1 and Rap2 subfamilies that might play a role in the regulation of cell matrix adhesion during cellular functions that are critical for physiological and pathophysiological processes, such as cell migration.

5 Materials

5.1 Devices and Equipment

8-well LabTek® chambers No. 1.0	Thermofischer Scientific
35-mm MatTek petri dishes No 1.5	MatTek Corporation
Agarose gel electrophoresis system	Bio-rad
Cell Culture dishes	Sarstedt
CellXpert Cell Culture Incubator	Eppendorf
Centrifuge 5810R	Eppendorf
Centrifuge 5415R	Eppendorf
Falcon tubes	Sarstedt
Microwave	Sharp
NALGENE™ Cryo 1°C freezing chamber	Thermofisher Scientific
Nanodrop 2000 Spectrophotometer	Thermofischer Scientific
NUAIRE™ class II biological safety cabinet	Integra Biosciences
Parafilm®	Bemis
Purelab flex 2 Water purification system	Elga
CFX 384™ Real-Time System	Bio-Rad
Research Plus Pipettes	Eppendorf
SafeSeal microfuge tubes	Sarstedt
Serological pipettes	Sarstedt
Thermocycler, Mastercycler personal	Eppendorf
Thermocycler, SimpliAmp	Thermofisher Scientific
Thermomixer compact	Eppendorf
UVP GelSolo, M-20V Geldokumentationssystem	analytikjena
Vacusafe comfort vacuum pump	IBS Integra Bioscience
Vortex Genie 2 touch mixer	Scientific Industries
Water bath	Köttermann

5.2 Kits

Gel Extraction Kit	Qiagen
GoScript™ Reverse Transcription System	Promega
GoTaq® qPCR System	Promega
Mini-Prep Kit	Qiagen

PCR Purification Kit	Qiagen
QIAshredder	Qiagen
RNase-free DNase Set	Qiagen
RNeasy Mini Kit	Qiagen

5.3 Chemicals

1 kb (+) DNA/ 100 bp ladder	New England Biolabs
2-mercaptoethanol	Sigma Aldrich
10x Buffer for KOD Hot Start DNA Polymerase	Novagen
Agarose	Roth
Ampicillin/ Carbenicillin	Roth
DAPI/ HOECHST 33342	Sigma Aldrich
dATP/dTTP/dCTP/dGTP/dNTP-Mix	New England Biolabs/ Novagen
DMEM (w phenol red)	PAN Biotech
DMEM (w/o phenol red)	PAN Biotech
DMSO anhydrous	Thermo Fisher
DPBS	PAN Biotech
EtBr (1% in ddH_20)	Gerbu
Ethanol	Roth
FBS	PAN Biotech, Sigma-Aldrich
Fibronectin	Sigma Aldrich
Glycerol	Sigma Aldrich
Goat anti-Mouse IgG (H+L) Cross-Adsorbed Secondary Antibody, Alexa Fluor™ 514	Thermofischer Scientific
Isopropanol	Roth
Kanamycin	Roth
L-Glutamine	PAN Biotech
Lipofectamin™ RNAiMax	Invitrogen
Lipofectamin™ 3000	Invitrogen
$MgCl_2$	New England Biolabs/ Novagen
NAD	New England Biolabs
ON-TARGETplus siRNAs	Dharmacon™, Horizon Discovery
OptiMEM	Gibco

PEG-8000	Promega
Purified Mouse Anti-Paxillin	BD Transduction Laboratories™
Purple Loading Dye	New England Biolabs
Restriction enzyme buffers	New England Biolabs
Rhodamin Phalloidin	Invitrogen
Tris-HCl	Sigma Aldrich

5.4 Enzymes

KOD Hot Start DNA Polymerase	Novagen
Phusion DNA polymerase	New England Biolabs
Q5 High-Fidelity DNA Polymerase	New England Biolabs
Restriction enzymes	New England Biolabs
Taq DNA ligase	New England Biolabs
Trypsin	PAN Biotech
T4 DNA ligase	New England Biolabs
T5 Exonuclease	New England Biolabs

5.5 Media and Buffer

TAE Buffer, 1x	40 mM Tris-Acetate, 1 mM EDTA, pH 8.3
A431 Culture Medium	DMEM, 1 % L-Glutamine, 10% FBS (filtered)
Imaging Medium	DMEM (w/o Phenol Red), 10 % FBS
Isothermal Buffer, 5x	25 % PEG-8000, 500 mM Tris-HCl (pH 7.5), 50 mM $MgCl_2$, 50 mM DTT, 1 mM each dATP/ dTTP/ dCTP/ dGTP, 5 mM NAD, H_2O
Gibson Master Mix	100 µL Isothermal Buffer 5x, 2 µL T5 Exonuclease (1 U/µL), 6.25 µL Phusion DNA Polymerase (2 U/µL), 50 µL Taq DNA Ligase (40 U/µL), 375 µL nfH2O
LB Medium	ddH2O, 5 g/L Yeast-Extract, 10 g/L NaCl, 10 g/L Tryptone (pH 7.4); Antibiotics: Kanamycin (50 µg/mL)
LB Agar Plates	LB Medium, 1.5 % Agar; Antibiotics: 50 mg/L Kanamycin
SOC Medium	2 % Bactotryptone, 0.5 % Yeast-Extract, 10 mM NaCl, 2.5 mM KCl, 10 mM MgCl2, 20 mM Glucose

5.6 Competent cells

XL10-Gold® Ultracompetent cells	Chemically competent E. coli (CaCl)
TOP10 Electrocomp™ E. coli	Electrocompetent E. coli
GH371	Chemically competent E. coli (CaCl)

5.7 Celllines

A431 (*Homo sapiens*, epidermoid carcinoma; AtCC-Nr.: CRL-1555)

6 Methods

6.1 Cell Culture

6.1.1 Technicalities

Maintenance of A431 cells (ATCC CRL-1555) was done using standard cell culture techniques, including 37°C and 5% CO_2 incubation and cultivation in DMEM medium (PAN Biotech; 10% FBS, Sigma-Aldrich Chemie GmbH/Merck; 2 mM L-Glutamine, PAN Biotech). Plasmid DNA transfection was performed with Lipofectamine™ 3000 reagent (Invitrogen). Imaging was performed on glass-bottom dishes freshly coated with fibronectin (10 µg/mL fibronectin, 45 min at RT). Depending on the experimental requirements, cells were either imaged shortly after replating (<6 hours) on MatTeks to investigate dynamic cell edge movements in highly migratory cells, or imaged after full cell attachment (>40 hours) on LabTek glass surface slides (Thermo Fischer Scientific), resulting in reduced edge dynamics and migration. Knockdown experiments were also performed on LabTek slides, where A431 cells were fixed and stained 3 or 8 hours after replating.

6.2 Molecular Biology

6.2.1 siRNA mediated knockdown

siRNA mediated knockdown was performed by transfecting 30 nM of ON-TARGETplus siRNAs (Dharmacon™, Horizon Discovery) into A431 cells using Lipofectamine™ RNAiMax (Invitrogen, Thermo Fisher Scientific). After an incubation period of 24h, cells were passaged to remove excess siRNAs (siControl: #2 5′-UGGUUUACAU GUUGUGUGA-3', Rap 1A: #5 5´-GAACAGAUUUUACGGGUUA-3´, #7 5´-GCGAGUAGUUGGCAAA GAG-3´). 48 hours after treatment, knockdown efficiency was assessed via qPCR.

6.2.2 RNA Isolation, cDNA synthesis, qPCR

RNA samples of A431 cells 48 hours post siRNA treatment were prepared using the RNeasy® Mini Kit (Qiagen) and the QIAshredder (Qiagen). cDNA synthesis was subsequently performed using the GoScript™ Reverse Transcription System (Promega). Evaluation of knockdown efficiency was assessed by qPCR. Hereby, PPIB (Peptidyl-prolyl isomerase B) served as a housekeeping gene, allowing measurement normalization for the individual mRNAs. Control treatments were performed using scrambled siRNA. Using the "GoTaq® qPCR System" Kit (Promega), qPCR reactions were setup with 300 mM of each primer, which were based on previously published sequences: Rap1A (Lin et al., 2015): TGTCTCACTGCACC TTCAATGGCAT (fw), ACGCCTCCTGAACCAAGGACCA (rv); Rap2B (Bruurs & Bos, 2014): GACTGATTGCGATTCTGAGG (fw), CACACTGTATTGGCATCAGT (rv); PPIB (Nazet et al., 2019): TTCCATCGTGTAATCAAGGACTTC (fw), GCTCACCGTAGATGCT CTTTC (rv).

6.2.3 Transformation of chemically competent E. coli

For each transformation reaction, 25 µL of chemically competent XL 10 Gold® ultracompetent *E. coli* cells are thawed on ice for 3 minutes, briefly centrifuged and then combined with up to 5 µL of plasmid DNA in a 1.5 mL Eppendorf Tube. Following 30 min incubation on ice, the cell suspension is heat shocked for 30 sec at 42 °C and then again cooled on ice for 5 additional min. Subsequently, 400 µL of 37°C prewarmed SOC medium are added and the *E. coli* cells are incubated at 37 °C for 1 hour at 500 rpm. The transformed cells are then spun down, 100 µL of the supernatant are taken up in a pipette while the remaining supernatant is discarded, and the cells are resuspended and plated entirely onto an antibiotic containing LB agar plate. For retransformation of previously prepared plasmids, 20 µL of the cell suspension are plated directly without prior centrifugation. The LB agar plates are incubated at 37 °C for 12-16 hours.

6.2.4 Preparation of liquid cultures and glycerol stocks

Liquid cultures are setup by inoculating LB medium containing a selective antibiotic by transferring a colony from an LB agar plate or transferring a small amount from a glycerol stock with a pipette tip. The cultures are then incubated at 37 °C overnight at 180 rpm. For glycerol stocks, 500 µL of a liquid culture in the exponential growing

phase are mixed with 500 µL of 50 % glycerol in a cryo-tube and then immediately stored at -80 °C.

6.2.5 Isolation of plasmid DNA from *E. coli*

Plasmid DNA was isolated from overnight liquid cultures using QIAprep Spin Miniprep Kit (Qiagen). To increase yield, the final elution step is performed with 30 µL of autoclaved ddH_2O and a prolonged incubation time of 5 min.

6.2.6 Measuring DNA and RNA concentration

Nucleic acid concentration was measured with a Nanodrop™ 2000 UV-Vis spectrophotometer at 260 nm after blanking with autoclaved ddH_2O.

6.2.7 Plasmid DNA sequencing

Sequencing of plasmid DNA was provided by Microsynth SeqLab. Sample preparation was performed according to the provided protocol. Primers were sent separately.

6.3 Microscopy

All microscopy experiments were performed with a TIRF microscope (Olympus IX-81 microscope; TIRF-MITICO motorized TIRF illumination combiner; Apo TIRF 60x/1.45 NA oil immersion objective; ZDC autofocus device), with exception of widefield tracking in single cell migration experiments (Olympus IX-81 microscope; UPlanSApo 10x/ air objective). Both microscopes are equipped with temperature-controlled (set to 37°C) incubation chambers without CO_2 control. Live-cell experiments were therefore performed in CO_2-independent medium (HEPES stabilized imaging medium, 10% FBS, PAN Biotech), and fixed cells were imaged in DPBS.

Single cell migration widefield imaging was performed using a 651 nm LED lamp (Spectra X light engine (Lumencor)).

For TIRF microscopy, a single dichroic mirror was employed (ZT405-440/514/561), combined with a matching set of emission filters (HC 435/40, HC 472/30, HC 542/27 and HC 629/53), an OBIS diode laser (514 nm, 150 mW; Coherent, Inc., Santa Clara, USA), and Cell R diode lasers (405 nm (50 mW); 445 nm (50 mW); 561 nm (100 mW) by Olympus). When necessary, widefield illumination (Spectra X light engine (Lumencor)) was performed in parallel to TIRF measurements. Detection was

performed with an EMCCD camera at medium gain without binning (C9100-13; Hamamatsu; Herrsching am Ammersee, Germany). Automatic scanning of the LabTek wells in morphometric analysis experiments was performed with wide-field illumination, software-based automated focusing and an UPlanSApo 10x/0.4 NA air objective.

For manually sorted live cell measurements, the only criterion to include cells into the analysis was adequate expression of all constructs and viability throughout the entire acquisition time-lapse.

6.3.1 Analysis of cell morphodynamics and local fluorescence signals at the cell edge

Measurement and analysis of cell morphodynamics was previously described in (Nanda et al., 2023). Activity sensors for Ras and Rap GTPases were transfected in combination with soluble fluorescent proteins as volume markers. Within the moving cell edges of transfected A431 cells, local enrichments of GTPase activity were detected automatically based on the volume markers which localization is ubiquitous and independent of the local changes in GTPase signal.
Quantification of these signals was also previously described in (Nanda et al., 2023). Briefly, a modified ADAPT plugin version (Barry et al., 2015) in combination with customized ImageJ analysis scripts allows generation of the depicted protrusion/ retraction enrichment measurements and the signal/ velocity cross-correlation functions. Here, a threshold of > 0.5 µm/min was set for cell edge movements to be considered protrusions, and a threshold of < -0.5 µm/min was set for the detection of retractions.

6.3.2 Analysis of Rac/Rap GTPase activity crosstalk via optogenetic perturbations

Optogenetic perturbations for GTPase activity crosstalk analysis were performed as described previously (Nanda et al., 2023). Here, the mCerulean-PA-Rac1 construct, which is a photo-activatable variant of the dominant positive Rac1 Q61L mutant, is transfected together with the activity sensor for the Rap GTPase, delCMV-mCitrine-2xRalGDS-GBD. TIRF illumination (445 nm Cell R diode laser) is used to activate Rac1 in a light-dependent fashion. A 10.000x neutral-density filter in the light path of the 445 nm TIRF illumination is used to prevent excess activation of PA-Rac1 and in addition, the neutral-density filter wheel built into the microscopy setup is set to 30 % to further

reduce illumination intensity. During the time range of photoactivation, the TIRF illumination at 445 nm was constantly on, with the exception of exposure times for active image acquisition to avoid crosstalk with measurements. After the experiment, an image with 445nm excitation was acquired to evaluate the expression of the mCerulean-PA-Rac1 construct.

Analysis of this experiment was also previously described in (Nanda et al., 2023). Measurement of the activity sensor in the whole cell adhesion area (A_{Rap}) was performed by subtracting the raw outside-the-cell background fluorescence intensity ($I_{Rap,BG}$) from the raw Rap activity sensor intensity measurements (I_{Rap}). These normalized values are divided by the background-corrected, initial intensity values ($I_{Rap,0} - I_{Rap,0,BG}$) from the timepoint before the light-based perturbation:

$$A_{Rap} = \frac{I_{Rap} - I_{Rap,BG}}{I_{Rap,0} - I_{Rap,0,BG}}$$

6.3.3 Analysis of Rap/ Rac GTPase activity crosstalk via photochemically-induced dimerization

Photochemically-induced dimerization for GTPase activity crosstalk analysis was performed as described previously (X. Chen et al., 2017). Photo-uncaging of the chemical NvocTMP-Cl dimerizer was introduced either locally or in the whole attachment area by either a single 405 nm illumination pulse (200 ms, 180 nW) within a diffraction-limited spot (FRAP mode of the build-in TIR-MITICO motorized TIRF illumination combiner) or in the entire cell attachment area via 405 nm TIRF illumination (200 ms, 540 nW). The laser power was detected at the aperture of the Apo TIRF 60x/1.45 NA oil immersion objective. The time series of perturbation and response fluorescence signals were quantified at the perturbation site after stabilization and background correction. Only the cells that showed ≥ 5% of perturbation fluorescence signal increase within 30 - 50 seconds after illumination were included in subsequent analysis to exclude cells in which the perturbation was weak.

6.3.4 Analysis of cell morphology

For the quantification of the cell attachment area, 15 k A431 cells were reseeded for every condition onto LabTek wells that were freshly coated with fibronectin (10 mg/mL) at 96 hours post siRNA transfection. 8 hours after reseeding, the cells were gently washed with 37° DPBS (400µL, 3x) and subsequently fixed with 37°C formaldehyde (200µL, 3.7 % in DPBS) for 20 min at 37°C. The cells were again washed with DPBS (3x) and afterwards permeabilized with Triton X-100 (200µL, 0.1% in DPBS) for 15 min at RT. Washing with DPBS (3x) was then followed by in-the-dark staining of the cells for F-actin (Rhodamin Phalloidin (200µL, 1:1000 in DPBS)) and nuclei (Hoechst 33342 (200µL, 1:1000 in DPBS)) for 30 min at RT. Stained cells were again washed with DPBS (3x), sealed air-tight with Parafilm® and then stored at 4 °C until imaging. Imaging was performed within 24 h of fixing, whereby the automated scanning of the individual wells yielded 64 images per condition.
These images were then analyzed to quantify the cell attachment area size with the image analysis software CellProfiler (Carpenter et al., 2006). Here, primary objects were the nuclei, that were detected based on the Hoechst staining signals and an adaptive Otsu thresholding (two classes, typical object diameter set to 5-25 pixels). Cells were detected as secondary objects based on the Rhodamin Phalloidin staining signals. This was performed by employing the detected nuclei as the input objects and using the propagation method and Otsu thresholding (global three class). The reported cell attachment area was determined as the area of the secondary objects.

For the quantification of focal adhesion formation, 15 k A431 cells were reseeded for each condition onto LabTek wells that were freshly coated with fibronectin (10 mg/mL) at 96 hours post siRNA transfection. 3 and 8 hours after reseeding, the cells were gently washed with 37° DPBS (400µL, 3x) and subsequently fixed with 37°C formaldehyde (200µL, 3.7 % in DPBS) for 20 min at 37°C. The cells were again washed with DPBS (3x) and afterwards permeabilized with Triton X-100 (200µL, 0.1% in DPBS) for 15 min at RT. After washing the cells with DPBS (3x), blocking was performed with BSA (200µL, 2 % in DPBS) for 1 hour at RT, and subsequently the cells were incubated with the primary antibody (200 µL, Purified Mouse Anti-Paxillin (Clone 349), BD Transduction Laboratories™, Cat 610051, 1:400 in 2% BSA/DPBS) for 1 hour at RT. Washing with DPBS (3x) was then followed by staining of the cells for F-actin (Rhodamin Phalloidin (200µL, 1:1000 in DPBS)) and nuclei (Hoechst 33342 (200µL,

1:1000 in DPBS)) in combination with the secondary antibody (Goat Anti-Mouse IgG, Alexa Fluor™ 514, Invitrogen, Cat A-31555, 1:1000 in 2% BSA/DPBS,) for 1 hour at RT in the dark. Stained cells were again washed with DPBS (3x), sealed air-tight with Parafilm® and then stored at 4 °C until imaging. Imaging was performed within 24 h of fixing. Manual imaging of the individual wells yielded >20 images per condition, that each had 40 – 60 % cell coverage.

These images were then again analyzed with the software CellProfiler (Carpenter et al., 2006). Here, the cell adhesion area size, the maximal paxillin signal intensity and the percentage of focal adhesion area in comparison to the complete attachment area was assessed. Initially, a median filter (window size of 3 pixels) was applied to the Hoechst-stained nuclei images to increase contrast. Subsequently, a morphological tophat filter as well as a disk structuring element with a size of 25 pixels was applied together with background suppression (feature size of 25 pixels). Using these contrast enhanced images, the nuclei were then detected as primary objects by applying a manual threshold (0.005) and a typical object diameter (10-500 pixel). Cells were again detected as secondary objects by using the widefield paxillin-staining images, as these were dominated by intense cytosolic signals. Hereby, the nuclei primary objects were used as input objects, and extrapolation of the cell body was performed with the propagation method and an adaptive Sauvola thresholding. The attachment area was again determined by quantification of the secondary cell object area size. Within the TIRF paxillin images, the focal adhesion structures of common size were enhanced (speckle method, feature size: 6 pixels) and then used as basis for identification of additional primary objects (typical diameter: 5 - 100, manual threshold 0.05). These focal adhesion objects were subsequently set as child objects for the overlapping and thereby corresponding secondary objects, the cells. The described staining signal intensity of these focal adhesion objects were determined in the original paxillin images (TIRF), and their size was measured using the focal adhesion primary objects.

6.3.5 Analysis of random migration

To investigate the effect of Rap knockdown on migration behavior, 10k A431 cells were seeded in each well of a fibronectin coated 8-well LabTek dish at 96 hours post siRNA transfection. 6 hours after seeding, nuclei staining is performed by incubation with DMSO diluted SPY650-DNA dye (Spirochrome, 1:1000 in imaging medium) for 1.5 hours. The cells are washed with imaging medium once and incubated for an additional

hour before the automated imaging is set up with a frame rate of 1/min. Using the TrackMate Plugin in Fiji, the stained nuclei are tracked automatically, and the generated data are further processed using Excel Macros (Direction Autocorrelation) and the Fiji plugin Chemotaxis (Ibidi GmbH, Martinsried, Germany). Only cells that remain in the field of view for the entire imaging time are included in the analysis.

6.3.6 Software for image and video analysis

Analysis of microscopy images and videos was performed with the software FIJI (https://imagej.net/software/fiji/), including its Kymograph and image stabilizer plugins (K. Li & Kang, 2008), a modified version of the ADAPT plugin (Barry et al., 2015; Nanda et al., 2023), the TrackMate as well as the Chemotaxis plugin. Cell adhesion area calculation was performed using Cell Profiler (Carpenter et al., 2006), and further data processing was performed in MatLab. Migration data were processed using Excel macros (Direction autocorrelation). Plotting and statistical analyses were performed in Prism (GraphPad). Values of individual conditions were compared to the expected value “0” in one sample t-tests, based on the null hypothesis (Figure 9m-o). All other statistical tests used the student´s t-test to compare two conditions; and the one-way ANOVA analysis and Dunnet’s post-test were used for comparison of more than two conditions.

6.3.7 Use of AI in this thesis

The AI writing assistant DeepL Write (*DeepL Write*, 2022) was used to optimize text for grammar and clarity.

7 References

Abram, C. L., & Lowell, C. A. (2009). Leukocyte adhesion deficiency syndrome: a controversy solved. *Immunology and Cell Biology*, *87*(6), 440–442. https://doi.org/10.1038/ICB.2009.32

Alanko, J., Uçar, M. C., Canigova, N., Stopp, J., Schwarz, J., Merrin, J., Hannezo, E., & Sixt, M. (2023). CCR7 acts as both a sensor and a sink for CCL19 to coordinate collective leukocyte migration. *Science Immunology*, *8*(87). https://doi.org/10.1126/SCIIMMUNOL.ADC9584

Alexandrova, A. Y., Chikina, A. S., & Svitkina, T. M. (2020). Actin cytoskeleton in mesenchymal-to-amoeboid transition of cancer cells. *International Review of Cell and Molecular Biology*, *356*, 197. https://doi.org/10.1016/BS.IRCMB.2020.06.002

Alpha, K. M., Xu, W., & Turner, C. E. (2020). Paxillin family of focal adhesion adaptor proteins and regulation of cancer cell invasion. *International Review of Cell and Molecular Biology*, *355*, 1. https://doi.org/10.1016/BS.IRCMB.2020.05.003

Ananthakrishnan, R., & Ehrlicher, A. (2007). The Forces Behind Cell Movement. *International Journal of Biological Sciences*, *3*(5), 303–317. https://doi.org/10.7150/IJBS.3.303

Artemenko, Y., Niu, G., Arnold, M. E., Roberts, K. E., Fernandez, B. N., Flores, T., McClave, H. D., Paestella, M., Borleis, J., & Devreotes, P. N. (2025). A negative feedback loop between small GTPase Rap1 and mammalian tumor suppressor homologue KrsB regulates cell-substrate adhesion in Dictyostelium. *Molecular Biology of the Cell*, *36*(4). https://doi.org/10.1091/MBC.E24-11-0507

Arthur, W. T., Quilliam, L. A., & Cooper, J. A. (2004). Rap1 promotes cell spreading by localizing Rac guanine nucleotide exchange factors. *The Journal of Cell Biology*, *167*(1), 111. https://doi.org/10.1083/JCB.200404068

Aznavoorian, S., Stracke, M. L., Krutzsch, H., Schiffmann, E., & Liotta, L. A. (1990). Signal transduction for chemotaxis and haptotaxis by matrix molecules in tumor cells. *The Journal of Cell Biology*, *110*(4), 1427–1438. https://doi.org/10.1083/JCB.110.4.1427

Bailey, C. L., Kelly, P., & Casey, P. J. (2009). Activation of Rap1 promotes prostate cancer metastasis. *Cancer Research*, *69*(12), 4962–4968. https://doi.org/10.1158/0008-5472.CAN-08-4269

Barry, D. J., Durkin, C. H., Abella, J. V., & Way, M. (2015). Open source software for quantification of cell migration, protrusions, and fluorescence intensities. *Journal of Cell Biology*, *209*(1), 163–180. https://doi.org/10.1083/JCB.201501081/VIDEO-3

Bar-Sagi, D., & Hall, A. (2000). Ras and Rho GTPases: A family reunion. *Cell*, *103*(2), 227–238. https://doi.org/10.1016/S0092-8674(00)00115-X/ASSET/C68AC61B-8391-4F81-9CCF-BFE307677C26/MAIN.ASSETS/GR6.JPG

Bear, J. E., Rawls, J. F., & Saxe, C. L. (1998). SCAR, a WASP-related Protein, Isolated as a Suppressor of Receptor Defects in Late Dictyostelium Development. *The Journal of Cell Biology*, *142*(5), 1325. https://doi.org/10.1083/JCB.142.5.1325

Boettner, B., & Van Aelst, L. (2009). Control of cell adhesion dynamics by Rap1 signaling. *Current Opinion in Cell Biology*, *21*(5), 684–693. https://doi.org/10.1016/J.CEB.2009.06.004

Bosgraaf, L., & Van Haastert, P. J. M. (2009). The Ordered Extension of Pseudopodia by Amoeboid Cells in the Absence of External Cues. *PLOS ONE*, *4*(4), e5253. https://doi.org/10.1371/JOURNAL.PONE.0005253

Bruurs, L. J. M., & Bos, J. L. (2014). Mechanisms of Isoform Specific Rap2 Signaling during Enterocytic Brush Border Formation. *PLoS ONE*, *9*(9), e106687. https://doi.org/10.1371/JOURNAL.PONE.0106687

Burute, M., & Thery, M. (2012). Spatial segregation between cell–cell and cell–matrix adhesions. *Current Opinion in Cell Biology*, *24*(5), 628–636. https://doi.org/10.1016/J.CEB.2012.07.003

Calderon, A. (2014). *Acute Perturbation and Activity Measurement of Rho GTPases in Living Cells.* [Dissertation]. TU Dortmund.

Carpenter, A. E., Jones, T. R., Lamprecht, M. R., Clarke, C., Kang, I. H., Friman, O., Guertin, D. A., Chang, J. H., Lindquist, R. A., Moffat, J., Golland, P., & Sabatini, D. M. (2006). CellProfiler: Image analysis software for identifying and quantifying cell phenotypes. *Genome Biology*, *7*(10), 1–11. https://doi.org/10.1186/GB-2006-7-10-R100/FIGURES/4

Case, L. B., & Waterman, C. M. (2015). Integration of actin dynamics and cell adhesion by a three-dimensional, mechanosensitive molecular clutch. *Nature Cell Biology*, *17*(8), 955–963. https://doi.org/10.1038/NCB3191

Chen, B., Chou, H. T., Brautigam, C. A., Xing, W., Yang, S., Henry, L., Doolittle, L. K., Walz, T., & Rosen, M. K. (2017). Rac1 GTPase activates the WAVE regulatory complex through two distinct binding sites. *ELife*, *6*, e29795. https://doi.org/10.7554/ELIFE.29795

Chen, X., Venkatachalapathy, M., Kamps, D., Weigel, S., Kumar, R., Orlich, M., Garrecht, R., Hirtz, M., Niemeyer, C. M., Wu, Y. W., & Dehmelt, L. (2017). “Molecular Activity Painting”: Switch-like, Light-Controlled Perturbations inside Living Cells. *Angewandte Chemie International Edition*, *56*(21), 5916–5920. https://doi.org/10.1002/ANIE.201611432

Chi, X., Wang, S., Huang, Y., Stamnes, M., & Chen, J. L. (2013). Roles of Rho GTPases in Intracellular Transport and Cellular Transformation. *International Journal of Molecular Sciences*, *14*(4), 7089. https://doi.org/10.3390/IJMS14047089

Chiu, V. K., Bivona, T., Hach, A., Sajous, J. B., Silletti, J., Wiener, H., Johnson, R. L., Cox, A. D., & Philips, M. R. (2002). Ras signalling on the endoplasmic reticulum and the Golgi. *Nature Cell Biology 2002 4:5*, *4*(5), 343–350. https://doi.org/10.1038/ncb783

Cooper, G. M. (2000). *The Cytoskeleton and Cell Movement*. https://www.ncbi.nlm.nih.gov/books/NBK9893/

De Pascalis, C., & Etienne-Manneville, S. (2017). Single and collective cell migration: the mechanics of adhesions. *Molecular Biology of the Cell*, *28*(14), 1833. https://doi.org/10.1091/MBC.E17-03-0134

DeepL Write. (2022). https://www.deepl.com/de/write

Devreotes, P. N., Bhattacharya, S., Edwards, M., Iglesias, P. A., Lampert, T., & Miao, Y. (2017). Excitable Signal Transduction Networks in Directed Cell Migration. *Annual Review of Cell and Developmental Biology*, *33*, 103. https://doi.org/10.1146/ANNUREV-CELLBIO-100616-060739

Diekmann, D., Abo, A., Johnston, C., Segal, A. W., Hallt, A., Diekmann, D., Johnston, C., Hall, A., Abo, A., & Segal, A. W. (1994). Interaction of Rac with p67phox and Regulation pf Phagocytic NADPH Oxidase Activity. *Science*, *265*(5171), 531–533. https://doi.org/10.1126/SCIENCE.8036496

Doyle, A. D., & Lee, J. (2005). Cyclic changes in keratocyte speed and traction stress arise from Ca2+-dependent regulation of cell adhesiveness. *Journal of Cell Science*, *118*(Pt 2), 369–379. https://doi.org/10.1242/JCS.01590

Drosten, M., Dhawahir, A., Sum, E. Y. M., Urosevic, J., Lechuga, C. G., Esteban, L. M., Castellano, E., Guerra, C., Santos, E., & Barbacid, M. (2010). Genetic analysis of Ras signalling pathways in cell proliferation, migration and survival. *The EMBO Journal*, *29*(6), 1091–1104. https://doi.org/10.1038/EMBOJ.2010.7

Euteneuer, U., & Schliwa, M. (1984). Persistent, directional motility of cells and cytoplasmic fragments in the absence of microtubules. *Nature 1984 310:5972*, *310*(5972), 58–61. https://doi.org/10.1038/310058a0

Ferro, E., Goitre, L., Baldini, E., Retta, S. F., & Trabalzini, L. (2014). Ras GTPases are both regulators and effectors of redox agents. *Methods in Molecular Biology (Clifton, N.J.)*, *1120*, 55–74. https://doi.org/10.1007/978-1-62703-791-4_5

Friedl, P., & Gilmour, D. (2009). Collective cell migration in morphogenesis, regeneration and cancer. *Nature Reviews Molecular Cell Biology 2009 10:7*, *10*(7), 445–457. https://doi.org/10.1038/nrm2720

Friedl, P., & Wolf, K. (2009). *Proteolytic interstitial cell migration: a five-step process*. https://doi.org/10.1007/s10555-008-9174-3

Gandalovičová, A., Vomastek, T., Rosel, D., & Brábek, J. (2016). Cell polarity signaling in the plasticity of cancer cell invasiveness. *Oncotarget*, *7*(18), 25022. https://doi.org/10.18632/ONCOTARGET.7214

Geiger, B., Spatz, J. P., & Bershadsky, A. D. (2009). Environmental sensing through focal adhesions. *Nature Reviews Molecular Cell Biology 2009 10:1*, *10*(1), 21–33. https://doi.org/10.1038/nrm2593

Gloerich, M., & Bos, J. L. (2011). Regulating Rap small G-proteins in time and space. *Trends in Cell Biology*, *21*(10), 615–623. https://doi.org/10.1016/J.TCB.2011.07.001

Grada, A., Otero-Vinas, M., Prieto-Castrillo, F., Obagi, Z., & Falanga, V. (2017). Research Techniques Made Simple: Analysis of Collective Cell Migration Using the Wound Healing Assay. *The Journal of Investigative Dermatology*, *137*(2), e11–e16. https://doi.org/10.1016/J.JID.2016.11.020

Graessl, M., Koch, J., Calderon, A., Kamps, D., Banerjee, S., Mazel, T., Schulze, N., Jungkurth, J. K., Patwardhan, R., Solouk, D., Hampe, N., Hoffmann, B., Dehmelt, L., & Nalbant, P. (2017). An excitable Rho GTPase signaling network generates dynamic subcellular contraction patterns. *The Journal of Cell Biology*, *216*(12), 4271–4285. https://doi.org/10.1083/JCB.201706052

Guilluy, C., Garcia-Mata, R., & Burridge, K. (2011). Rho protein crosstalk: another social network? *Trends in Cell Biology*, *21*(12), 718–726. https://doi.org/10.1016/J.TCB.2011.08.002

Guo, X. X., An, S., Yang, Y., Liu, Y., Hao, Q., & Xu, T. R. (2016). Rap-Interacting Proteins are Key Players in the Rap Symphony Orchestra. *Cellular Physiology and Biochemistry*, *39*(1), 137–156. https://doi.org/10.1159/000445612

Gupton, S. L., & Waterman-Storer, C. M. (2006). Spatiotemporal feedback between actomyosin and focal-adhesion systems optimizes rapid cell migration. *Cell*, *125*(7), 1361–1374. https://doi.org/10.1016/J.CELL.2006.05.029

Hanahan, D. (2022). Hallmarks of Cancer: New Dimensions. *Cancer Discovery*, *12*(1), 31–46. https://doi.org/10.1158/2159-8290.CD-21-1059

Holle, A. W., Govindan, N., Devi, K., Clar, K., Fan, A., Saif, T., Kemkemer, R., & Spatz, J. P. (2019). *Cancer Cells Invade Confined Microchannels via a Self-Directed Mesenchymal-to-Amoeboid Transition*. https://doi.org/10.1021/acs.nanolett.8b04720

Horwitz, R., & Webb, D. (2003). Cell migration. *Current Biology : CB*, *13*(19), R756–R759. https://doi.org/10.1016/j.cub.2003.09.014

Ipiña, E. P., d'Allesandro, J., Ladoux, B., & Camley, B. A. (2023). Secreted footprints let cells switch between confined, oscillatory, and exploratory migration. *BioRxiv*, 2023.09.14.557437. https://doi.org/10.1101/2023.09.14.557437

Janiszewska, M., Primi, M. C., & Izard, T. (2020). Cell adhesion in cancer: Beyond the migration of single cells. *The Journal of Biological Chemistry*, *295*(8), 2495. https://doi.org/10.1074/JBC.REV119.007759

Jansen, K. A., Atherton, P., & Ballestrem, C. (2017). Mechanotransduction at the cell-matrix interface. *Seminars in Cell & Developmental Biology*, *71*, 75–83. https://doi.org/10.1016/J.SEMCDB.2017.07.027

Jaśkiewicz, A., Pajką, B., & Orzechowski, A. (2018). The Many Faces of Rap1 GTPase. *International Journal of Molecular Sciences*, *19*(10), 2848. https://doi.org/10.3390/IJMS19102848

Joshi, M. S., Stanoev, A., Huebinger, J., Soetje, B., Zorina, V., Roßmannek, L., Michel, K., Müller, S. A., & Bastiaens, P. I. (2023). The EGFR phosphatase RPTPγ is a redox-regulated suppressor of promigratory signaling . *The EMBO Journal*, *42*(10). https://doi.org/10.15252/EMBJ.2022111806/SUPPL_FILE/EMBJ2022111806-SUP-0003-MOVIEEV1.ZIP

Kamps, D., & Dehmelt, L. (2017). *Deblurring Signal Network Dynamics*. https://doi.org/10.1021/acschembio.7b00451

Kamps, D., Koch, J., Juma, V. O., Campillo-Funollet, E., Graessl, M., Banerjee, S., Mazel, T., Chen, X., Wu, Y. W., Portet, S., Madzvamuse, A., Nalbant, P., & Dehmelt, L. (2020). Optogenetic Tuning Reveals Rho Amplification-Dependent

Dynamics of a Cell Contraction Signal Network. *Cell Reports*, *33*(9). https://doi.org/10.1016/J.CELREP.2020.108467

Kitagishi, Y., & Matsuda, S. (2013). RUFY, Rab and Rap Family Proteins Involved in a Regulation of Cell Polarity and Membrane Trafficking. *International Journal of Molecular Sciences 2013, Vol. 14, Pages 6487-6498*, *14*(3), 6487–6498. https://doi.org/10.3390/IJMS14036487

Klijn, C., Durinck, S., Stawiski, E. W., Haverty, P. M., Jiang, Z., Liu, H., Degenhardt, J., Mayba, O., Gnad, F., Liu, J., Pau, G., Reeder, J., Cao, Y., Mukhyala, K., Selvaraj, S. K., Yu, M., Zynda, G. J., Brauer, M. J., Wu, T. D., … Zhang, Z. (2014). A comprehensive transcriptional portrait of human cancer cell lines. *Nature Biotechnology 2014 33:3*, *33*(3), 306–312. https://doi.org/10.1038/nbt.3080

Lafuente, E. M., van Puijenbroek, A. A. F. L., Krause, M., Carman, C. V., Freeman, G. J., Berezovskaya, A., Constantine, E., Springer, T. A., Gertler, F. B., & Boussiotis, V. A. (2004). RIAM, an Ena/VASP and Profilin ligand, interacts with Rap1-GTP and mediates Rap1-induced adhesion. *Developmental Cell*, *7*(4), 585–595. https://doi.org/10.1016/J.DEVCEL.2004.07.021

Lagarrigue, F., Kim, C., & Ginsberg, M. H. (2016). The Rap1-RIAM-talin axis of integrin activation and blood cell function. *Blood*, *128*(4), 479. https://doi.org/10.1182/BLOOD-2015-12-638700

Lambert, J. M., Lambert, Q. T., Reuther, G. W., Malliri, A., Siderovski, D. P., Sondek, J., Collard, J. G., & Der, C. J. (2002). Tiam1 mediates Ras activation of Rac by a PI(3)K-independent mechanism. *Nature Cell Biology 2002 4:8*, *4*(8), 621–625. https://doi.org/10.1038/ncb833

Li, K., & Kang, S. (2008, February). *Image stabilizer*. https://www.cs.cmu.edu/~kangli/code/Image_Stabilizer.html

Li, Y., Grenklo, S., Higgins, T., & Karlsson, R. (2008). The profilin:actin complex localizes to sites of dynamic actin polymerization at the leading edge of migrating cells and pathogen-induced actin tails. *European Journal of Cell Biology*, *87*(11), 893–904. https://doi.org/10.1016/J.EJCB.2008.06.003

Lin, K. T., Yeh, Y. M., Chuang, C. M., Yang, S. Y., Chang, J. W., Sun, S. P., Wang, Y. S., Chao, K. C., & Wang, L. H. (2015). Glucocorticoids mediate induction of microRNA-708 to suppress ovarian cancer metastasis through targeting Rap1B. *Nature Communications 2015 6:1*, *6*(1), 1–13. https://doi.org/10.1038/ncomms6917

Looi, C. K., Hii, L. W., Ngai, S. C., Leong, C. O., & Mai, C. W. (2020). The Role of Ras-Associated Protein 1 (Rap1) in Cancer: Bad Actor or Good Player? *Biomedicines*, *8*(9), 334. https://doi.org/10.3390/BIOMEDICINES8090334

Lundquist, E. A. (2009). The Finer Points of Filopodia. *PLoS Biology*, *7*(6), e1000142. https://doi.org/10.1371/JOURNAL.PBIO.1000142

Luster, A. D., Alon, R., & von Andrian, U. H. (2005). Immune cell migration in inflammation: present and future therapeutic targets. *Nature Immunology 2005 6:12*, *6*(12), 1182–1190. https://doi.org/10.1038/ni1275

Lüttig, R., Nanda, S., Chandran, H. T., & Dehmelt, L. (2025). Crosstalk between Rac and Rap GTPases in migrating cells. *Molecular Biology of the Cell*. https://doi.org/10.1091/MBC.E25-02-0058

Machida, N., Umikawa, M., Takei, K., Sakima, N., Myagmar, B. E., Taira, K., Uezato, H., Ogawa, Y., & Kariya, K. I. (2004). Mitogen-activated Protein Kinase Kinase Kinase Kinase 4 as a Putative Effector of Rap2 to Activate the c-Jun N-terminal Kinase. *Journal of Biological Chemistry*, *279*(16), 15711–15714. https://doi.org/10.1074/jbc.C300542200

Mattila, P. K., & Lappalainen, P. (2008). Filopodia: molecular architecture and cellular functions. *Nature Reviews Molecular Cell Biology 2008 9:6*, *9*(6), 446–454. https://doi.org/10.1038/nrm2406

Medalia, O., Beck, M., Ecke, M., Weber, I., Neujahr, R., Baumeister, W., & Gerisch, G. (2007). Organization of actin networks in intact filopodia. *Current Biology : CB*, *17*(1), 79–84. https://doi.org/10.1016/J.CUB.2006.11.022

Mejillano, M. R., Kojima, S. I., Applewhite, D. A., Gertler, F. B., Svitkina, T. M., & Borisy, G. G. (2004). Lamellipodial Versus Filopodial Mode of the Actin

Nanomachinery: Pivotal Role of the Filament Barbed End. *Cell*, *118*(3), 363–373. https://doi.org/10.1016/J.CELL.2004.07.019

Miao, F., Cui, C., Zuo, D., Zhang, H., Mei, P., Chen, H., Wei, S., Yang, F., Zheng, J., Bai, J., & Fan, Y. (2019). Rap2B promotes cell adhesion, proliferation, migration and invasion of human glioma. *Journal of Neuro-Oncology*, *143*(2), 221–229. https://doi.org/10.1007/S11060-019-03163-6/FIGURES/4

Michaelis, U. R. (2014). Mechanisms of endothelial cell migration. *Cellular and Molecular Life Sciences: CMLS*, *71*(21), 4131. https://doi.org/10.1007/S00018-014-1678-0

Miertzschke, M., Stanley, P., Bunney, T. D., Rodrigues-Lima, F., Hogg, N., & Katan, M. (2007). Characterization of Interactions of Adapter Protein RAPL/Nore1B with RAP GTPases and Their Role in T Cell Migration * □ S. *Journal of Biological Chemistry*, *282*, 30629–30642. https://doi.org/10.1074/jbc.M704361200

Miller, K. G. (2002). Extending the Arp2/3 complex and its regulation beyond the leading edge. *Journal of Cell Biology*, *156*(4), 591–593. https://doi.org/10.1083/JCB.200201107

Moreau, H. D., Piel, M., Voituriez, R., & Lennon-Duménil, A. M. (2018). Integrating Physical and Molecular Insights on Immune Cell Migration. *Trends in Immunology*, *39*(8), 632–643. https://doi.org/10.1016/J.IT.2018.04.007/ASSET/981DFE25-5914-4805-8C02-B10D27E07BE3/MAIN.ASSETS/GR3.JPG

Nalbant, P., & Dehmelt, L. (2018). Exploratory cell dynamics: A sense of touch for cells? *Biological Chemistry*, *399*(8), 809–819. https://doi.org/10.1515/HSZ-2017-0341/ASSET/GRAPHIC/J_HSZ-2017-0341_FIG_004.JPG

Nalbant, P., Wagner, J., & Dehmelt, L. (2023). Direct investigation of cell contraction signal networks by light-based perturbation methods. *Pflugers Archiv European Journal of Physiology*, *475*(12), 1439–1452. https://doi.org/10.1007/S00424-023-02864-2

Nanda, S. (2023). *Investigation of signal networks that control dynamic cell shape changes* [Dissertation of Suchet Nanda, TU Dortmund]. https://eldorado.tu-

dortmund.de/server/api/core/bitstreams/42a6e8a4-0186-47e8-9d17-044f005f60a6/content

Nanda, S., Calderon, A., Sachan, A., Duong, T. T., Koch, J., Xin, X., Solouk-Stahlberg, D., Wu, Y. W., Nalbant, P., & Dehmelt, L. (2023). Rho GTPase activity crosstalk mediated by Arhgef11 and Arhgef12 coordinates cell protrusion-retraction cycles. *Nature Communications 2023 14:1*, *14*(1), 1–17. https://doi.org/10.1038/s41467-023-43875-y

Nazet, U., Schröder, A., Grässel, S., Muschter, D., Proff, P., & Kirschneck, C. (2019). Housekeeping gene validation for RT-qPCR studies on synovial fibroblasts derived from healthy and osteoarthritic patients with focus on mechanical loading. *PLOS ONE*, *14*(12), e0225790. https://doi.org/10.1371/JOURNAL.PONE.0225790

Nicholson-Dykstra, S., Higgs, H. N., & Harris, E. S. (2005). Actin Dynamics: Growth from Dendritic Branches. *Current Biology*, *15*(9), R346–R357. https://doi.org/10.1016/J.CUB.2005.04.029

Niculescu, I., Textor, J., & de Boer, R. J. (2015). Crawling and Gliding: A Computational Model for Shape-Driven Cell Migration. *PLoS Computational Biology*, *11*(10). https://doi.org/10.1371/JOURNAL.PCBI.1004280

Novikov, N. M., Zolotaryova, S. Y., Gautreau, A. M., & Denisov, E. V. (2020). Mutational drivers of cancer cell migration and invasion. *British Journal of Cancer 2020 124:1*, *124*(1), 102–114. https://doi.org/10.1038/s41416-020-01149-0

Pankov, R., Endo, Y., Even-Ram, S., Araki, M., Clark, K., Cukierman, E., Matsumoto, K., & Yamada, K. M. (2005). A Rac switch regulates random versus directionally persistent cell migration. *Journal of Cell Biology*, *170*(5), 793–802. https://doi.org/10.1083/JCB.200503152

Pannekoek, W. J., Linnemann, J. R., Brouwer, P. M., Bos, J. L., & Rehmann, H. (2013). Rap1 and Rap2 antagonistically control endothelial barrier resistance. *PloS One*, *8*(2). https://doi.org/10.1371/JOURNAL.PONE.0057903

Pasapera, A. M., Schneider, I. C., Rericha, E., Schlaepfer, D. D., & Waterman, C. M. (2010). Myosin II activity regulates vinculin recruitment to focal adhesions through FAK-mediated paxillin phosphorylation. *Journal of Cell Biology*, *188*(6), 877–890. https://doi.org/10.1083/JCB.200906012/VIDEO-1

Plak, K., Veltman, D., Fusetti, F., Beeksma, J., Rivero, F., Van Haastert, P. J. M., & Kortholt, A. (2013). GxcC connects Rap and Rac signaling during Dictyostelium development. *BMC Cell Biology*, *14*(1), 6. https://doi.org/10.1186/1471-2121-14-6

Pollard, T. D., Blanchoin, L., & Mullins, R. D. (2001). Actin Dynamics. *Journal of Cell Science*, *114*(1), 3–4. https://doi.org/10.1242/JCS.114.1.3

Qiao, L., Zhang, Z. B., Zhao, W., Wei, P., & Zhang, L. (2022). Network design principle for robust oscillatory behaviors with respect to biological noise. *ELife*, *11*. https://doi.org/10.7554/ELIFE.76188

Raaijmakers, J. H., & Bos, J. L. (2009). Specificity in Ras and Rap Signaling. *The Journal of Biological Chemistry*, *284*(17), 10995. https://doi.org/10.1074/JBC.R800061200

Rodriguez-Viciana, P., Sabatier, C., & McCormick, F. (2004). Signaling Specificity by Ras Family GTPases Is Determined by the Full Spectrum of Effectors They Regulate. *Molecular and Cellular Biology*, *24*(11), 4943. https://doi.org/10.1128/MCB.24.11.4943-4954.2004

Rothenberg, K. E., Chen, Y., McDonald, J. A., & Fernandez-Gonzalez, R. (2023). Rap1 coordinates cell-cell adhesion and cytoskeletal reorganization to drive collective cell migration in vivo. *Current Biology*, *33*(13), 2587-2601.e5. https://doi.org/10.1016/J.CUB.2023.05.009

Scarpa, E., & Mayor, R. (2016). Collective cell migration in development. *The Journal of Cell Biology*, *212*(2), 143. https://doi.org/10.1083/JCB.201508047

Scrima, A., Thomas, C., Deaconescu, D., & Wittinghofer, A. (2008). The Rap-RapGAP complex: GTP hydrolysis without catalytic glutamine and arginine residues. *EMBO Journal*, *27*(7), 1145–1153.

https://doi.org/10.1038/EMBOJ.2008.30/SUPPL_FILE/EMBJ200830-SUP-0001.PDF

Seetharaman, S., & Etienne-Manneville, S. (2020). Cytoskeletal Crosstalk in Cell Migration Trends in Cell Biology. *Trends in Cell Biology*, *30*(9). https://doi.org/10.1016/j.tcb.2020.06.004

Shah, S., Brock, E. J., Ji, K., & Mattingly, R. R. (2018). Ras and Rap1: A Tale of Two GTPases. *Seminars in Cancer Biology*, *54*, 29. https://doi.org/10.1016/J.SEMCANCER.2018.03.005

Sheetz, M. P., Felsenfeld, D., Galbraith, C. G., & Choquet, D. (1999). Cell migration as a five-step cycle. *Biochemical Society Symposium*, *65*, 233–243. https://ohsu.elsevierpure.com/en/publications/cell-migration-as-a-five-step-cycle

Shimonaka, M., Katagiri, K., Nakayama, T., Fujita, N., Tsuruo, T., Yoshie, O., & Kinashi, T. (2003). Rap1 translates chemokine signals to integrin activation, cell polarization, and motility across vascular endothelium under flow. *The Journal of Cell Biology*, *161*(2), 417. https://doi.org/10.1083/JCB.200301133

Soriano, O., Alcón-Pérez, M., Vicente-Manzanares, M., & Castellano, E. (2021). The Crossroads between RAS and RHO Signaling Pathways in Cellular Transformation, Motility and Contraction. *Genes*, *12*(6), 819. https://doi.org/10.3390/GENES12060819

Stefanini, L., Boulaftali, Y., Ouellette, T. D., Holinstat, M., Désiré, L., Leblond, B., Andre, P., Conley, P. B., & Bergmeier, W. (2011). Rap1-Rac1 Circuits Potentiate Platelet Activation. *Arteriosclerosis, Thrombosis, and Vascular Biology*, *32*(2), 434. https://doi.org/10.1161/ATVBAHA.111.239194

Stinson, M. W., Liu, S., Laurenson, A. J., & Rotty, J. D. (2024). Macrophage migration is differentially regulated by fibronectin and laminin through altered adhesion and myosin II localization. *Molecular Biology of the Cell*, *35*(2), 1–20. https://doi.org/10.1091/MBC.E23-04-0137/ASSET/IMAGES/LARGE/MBC-35-AR22-G008.JPEG

Sunyer, R., & Trepat, X. (2020). Durotaxis. *Current Biology*, *30*(9), R383–R387. https://doi.org/10.1016/j.cub.2020.03.051

Svitkina, T. M., Bulanova, E. A., Chaga, O. Y., Vignjevic, D. M., Kojima, S. ichiro, Vasiliev, J. M., & Borisy, G. G. (2003). Mechanism of filopodia initiation by reorganization of a dendritic network. *Journal of Cell Biology*, *160*(3), 409–421. https://doi.org/10.1083/JCB.200210174

Theriot, J. A. (1997). Accelerating on a Treadmill: ADF/Cofilin Promotes Rapid Actin Filament Turnover in the Dynamic Cytoskeleton. *The Journal of Cell Biology*, *136*(6), 1165. https://doi.org/10.1083/JCB.136.6.1165

Trepat, X., Chen, Z., & Jacobson, K. (2012). Cell Migration. *Comprehensive Physiology*, *2*(4), 2369. https://doi.org/10.1002/CPHY.C110012

Vignjevic, D., Yarar, D., Welch, M. D., Peloquin, J., Svitkina, T., & Borisy, G. G. (2003). Formation of filopodia-like bundles in vitro from a dendritic network. *Journal of Cell Biology*, *160*(6), 951–962. https://doi.org/10.1083/JCB.200208059

Vitorino, P., Yeung, S., Crow, A., Bakke, J., Smyczek, T., West, K., McNamara, E., Eastham-Anderson, J., Gould, S., Harris, S. F., Ndubaku, C., & Ye, W. (2015). MAP4K4 regulates integrin-FERM binding to control endothelial cell motility. *Nature*, *519*(7544), 425–430. https://doi.org/10.1038/NATURE14323

Watanabe, N., & Mitchison, T. J. (2002). Single-molecule speckle analysis of actin filament turnover in lamellipodia. *Science*, *295*(5557), 1083–1086. https://doi.org/10.1126/SCIENCE.1067470/SUPPL_FILE/1067470S5_THUMB.GIF

Weeks, R., Mehta, S., & Zhang, J. (2024). Genetically encodable biosensors for Ras activity. *RSC Chemical Biology*, *5*(4), 312. https://doi.org/10.1039/D3CB00185G

Wehrle-Haller, B. (2013). *The Role of Integrins in Cell Migration*. https://www.ncbi.nlm.nih.gov/books/NBK6613/

Wollrab, V., Belmonte, J. M., Baldauf, L., Leptin, M., Nédeléc, F., & Koenderink, G. H. (2019). Polarity sorting drives remodeling of actin-myosin networks. *Journal of Cell Science*, *132*(4). https://doi.org/10.1242/JCS.219717/VIDEO-15

Wu, Y. I., Frey, D., Lungu, O. I., Jaehrig, A., Schlichting, I., Kuhlman, B., & Hahn, K. M. (2009). A genetically encoded photoactivatable Rac controls the motility of living cells. *Nature*, *461*(7260), 104–108. https://doi.org/10.1038/NATURE08241

Yamashita, S., Mochizuki, N., Ohba, Y., Tobiume, M., Okada, Y., Sawa, H., Nagashima, K., & Matsuda, M. (2000). CalDAG-GEFIII activation of Ras, R-ras, and Rap1. *The Journal of Biological Chemistry*, *275*(33), 25488–25493. https://doi.org/10.1074/JBC.M003414200

Yoshida, H., Okumura, N., Kitagishi, Y., Shirafuji, N., & Matsuda, S. (2010). Rab5(Q79L) interacts with the carboxyl terminus of RUFY3. *International Journal of Biological Sciences*, *6*(2), 187. https://doi.org/10.7150/IJBS.6.187

Zhang, B., Li, S., Ding, J., Guo, J., Ma, Z., & Duan, H. (2025). Rho-GTPases subfamily: cellular defectors orchestrating viral infection. *Cellular & Molecular Biology Letters 2025 30:1*, *30*(1), 1–27. https://doi.org/10.1186/S11658-025-00722-W

Zhang, H., Chang, Y. C., Brennan, M. L., & Wu, J. (2013). The structure of Rap1 in complex with RIAM reveals specificity determinants and recruitment mechanism. *Journal of Molecular Cell Biology*, *6*(2), 128. https://doi.org/10.1093/JMCB/MJT044

Zhang, Y. L., Wang, R. C., Cheng, K., Ring, B. Z., & Su, L. (2017). Roles of Rap1 signaling in tumor cell migration and invasion. *Cancer Biology & Medicine*, *14*(1), 90–99. https://doi.org/10.20892/J.ISSN.2095-3941.2016.0086

Zwartkruis, F. J. T., Wolthuis, R. M. F., Nabben, N. M. J. M., Franke, B., & Bos, J. L. (1998). Extracellular signal-regulated activation of Rap1 fails to interfere in Ras effector signalling. *The EMBO Journal*, *17*(20), 5905–5912. https://doi.org/10.1093/EMBOJ/17.20.5905

8 Appendix

8.1 Initial steps for the development of Rap1/Rap2 selective activity sensors

The proposed mechanism to generate opposite phenotypes by Rap1 vs Rap2 shown in Figure 14 is based on MAP4K4 as a specific Rap2 effector. To further investigate this idea, and to study the relative spatio-temporal activity patterns of Rap1 vs Rap2, a strategy was devised to distinguish these activities in living cells.

Unfortunately, effectors for the Ras/Rap family overlap substantially, making it difficult to design specific tools. For example, the RalGDS domain was chosen to generate the Rap sensor used in this study, because it preferentially binds Rap1a over Ras (Raaijmakers & Bos, 2009; Shah et al., 2018). The distinct activity patterns that substantially differ from the Ras sensor dynamics imply successful differentiation between Rap and Ras; however, the RalGDS-domain was previously suggested to bind strongly to both Rap1 and Rap2 isoforms (Rodriguez-Viciana et al., 2004). To experimentally determine the specificity of the RalGDS-domain based Rap sensor for Rap1 vs. Rap2, molecular activity painting was used (see Figure 16).

These experiments confirmed that the RalGDS-domain based Rap sensor binds to the active form of both Rap1a and of Rap2b: Perturbations with dominant positive mutants of these molecules both showed efficient recruitment of the RalGDS-domain-based activity sensor, while control constructs lacking the sensor domain did not show any response (Figure 16).

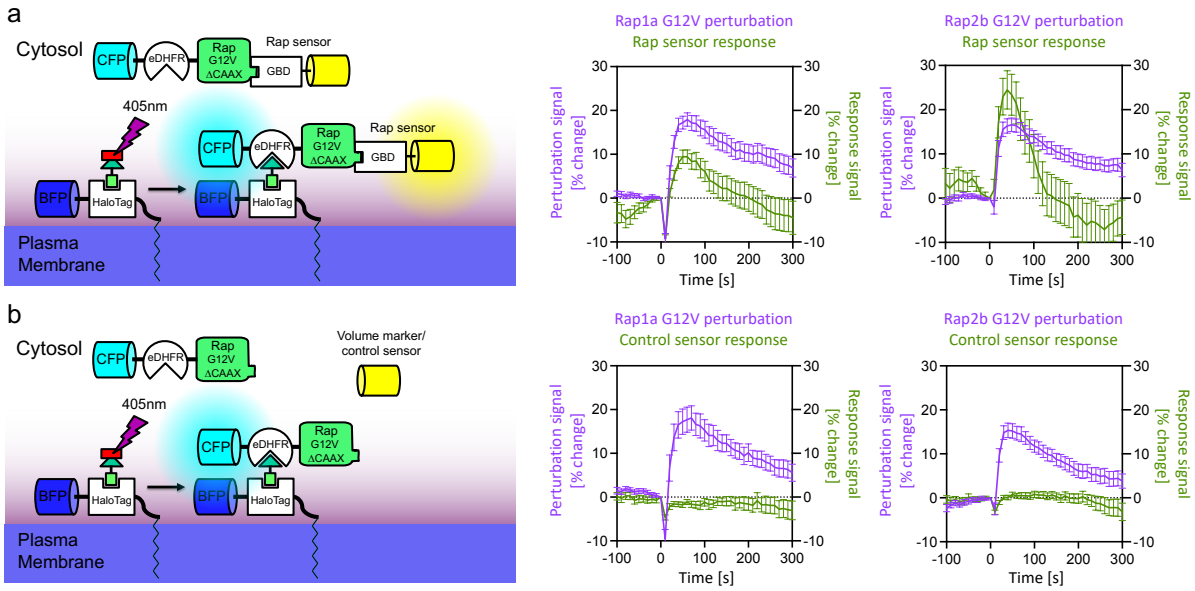

Figure 16: a-b) Quantification of local Rap1a and Rap2b perturbation and parallel measurement of Rap activity sensor (a) or control sensor recruitment dynamics (b). Contents for Rap1a G12V perturbation were reproduced from figure 7a and d for easier comparison. (a: n=19 for control and n=37 cells for the experimental condition, b: n=26 for control and n=26 cells for the experimental condition, from 3 independent experiments. Error bars represent the standard error of the mean (SEM).

To distinguish between active Rap1 and Rap2 in living cells, it would therefore be necessary to generate subfamily-specific sensors. This task poses quite a challenge, as many downstream effectors of Rap have not been assessed according to their specificity towards Rap1 vs Rap2 family proteins. Based on known effector domains specific for Rap2, three Rap2 specific candidate sensor constructs were generated: 1) A sensor based on the C-terminal Rap2-interacting CNH-domain of the effector MAP4K4 isoform 3, which was proposed to mediate Rap2-dependent negative regulation of cell adhesion, 2) A longer region of MAP4K4, that includes additional sequences N-terminal to the CNH domain from an alternatively spliced transcript (Machida et al., 2004), and 3) A sensor based on the RUN-domain of Rufy3, which was also proposed to be a Rap2-specific effector domain (Kitagishi & Matsuda, 2013; Yoshida et al., 2010).

Sensors based on just a single effector domain did not show any subcellular localization and did not show any significant enrichment in subcellular areas (data not shown). A similar observation was made with first generation Rap sensors based on a single RalGDS domain. At least one tandem repeat containing two RalGDS domains was necessary to detect Rap activity in cells, and therefore an analogous domain duplication was also performed for the prospective Rap2 sensors.

However, all generated sensor constructs were difficult to express in A431 cells and they showed little subcellular enrichment.

Future attempts to generate Rap1 or Rap2 specific sensors could start with a broader range of effector domains and benefit from the Molecular Activity Painting based Rap1a and Rap2b perturbation constructs to characterize their relative binding affinity to these isoforms.

8.2 Plasmid constructs

8.2.1 Plasmids used in this thesis

No.	Lab no.	Plasmid name	Source
1	162	delCMV-mCherry	Nanda et al., 2023
2	163	delCMV-mCitrine	Nanda et al., 2023
3	229	delCMV-mCherry-RBD	Calderon, 2014
4	239	mCerulean-PA-Rac-Q61L	Wu et al., 2009
5	323/ 956	mTurquoise2-NES-eDHFR-RhoAQ63L	Kamps et al., 2020
6	374/ 957	mTagBFP-HaloTag-CAAX	X. Chen et al., 2017
7	722	EYFP-C1 Rap 2A wt	Kind gift from Philippe Bastiaens (MPI Dortmund, Dep2 - Plasmid #2768)
8	725	ECFP-C1 Rap1B wt	Kind gift from Philippe Bastiaens (MPI Dortmund, Dep2 - Plasmid #2923)
9	727	EYFP-C1 Rap1A wt	Kind gift from Philippe Bastiaens (MPI Dortmund, Dep2 - Plasmid #2779)
10	778	delCMV-mCherry-3xp67Phox	Nanda et al., 2023

11	779	delCMV-2xRaf-GBD-mCherry	Lüttig et al., 2025
12	780	delCMV-mCitrine-2xRalGDS-GBD	Lüttig et al., 2025
13	804	delCMV-MCP-mCitrine-Rap1A-G12V	Nanda, 2023
14	908	mCherry-Rap2B	Addgene #118320
15	911	pDONR223-MAP4K4	Addgene #23486
16	943	nN_pcDNA3-mApple_empty_new	Kind gift from Perihan Nalbant (University Duisburg-Essen)

8.2.2 Plasmids generated in this thesis

No.	Lab no.	Plasmid name	Cloning method (Insert/ Vector, Lab no.)	Primer pair used	Enzymes used
1	844	delCMV_YFP_Rap1a	Restriction digest and ligation (727/162)	-	AgeI/ MfeI
2	845	delCMV_CFP_Rap1b	Restriction digest and ligation (725/162)	-	AgeI/ MfeI
3	846	delCMV_YFP_Rap2a	Restriction digest and ligation (722/ 162)	-	AgeI/ MfeI
4	918	delCMV_mCherry_Rufy3_RUND	Gibson assembly (Nested PCR of A431 cDNA/ 229)	1/ 2	MfeI/ BspEI

5	919	delCMV_mCherry_MAP4K4_CHD_long	Gibson assembly (911 “N_long”/ 911 “C_term”/ 229)	3 4	MfeI/ BspEI
6	920	delCMV_mCherry_MAP4K4_CHD_short	Gibson assembly (911 “N_short”/ 911 “C_term”/ 229)	5 4	MfeI/ BspEI
7	932	delCMV_mCherry_2x_Rufy3_RUND	Gibson assembly (918 PCR/ 918 RD)	6	BrsGI-HF
8	933	delCMV_mCherry_2x_MAP4K4_CHD_long	Gibson assembly (919 PCR/ 919 RD)	7	SgrAI
9	934	delCMV_mCherry_2x_MAP4K4_CHD_short	Gibson assembly (920 PCR/ 920 RD)	7	SgrAI
10	941	delCMV-mApple	Gibson assembly (943/ 162)	8/ 9	-
11	953	mCherry-Rap2B_G12V	Gibson assembly (908)	10/ 11	MluI/ AgeI
12	959	delCMV_mApple_1x_MAP4K4_CHD_long	Gibson assembly (943/ 919)	12/ 13	-
13	960	delCMV_mApple_2x_MAP4K4_CHD_long	Restriction digest and ligation (933/ 959)	-	BamHI-HF
14	961	mTurquoise2-NES-eDHFR-Rap1AG12V	Gibson assembly (RD free) (804/ 323)	14/ 15	-
15	962	mTurquoise2-NES-eDHFR-Rap2BG12V	Gibson assembly (RD free) (953/ 323)	16/ 17	-
16	987	delCMV-2xRaf-GBD-mCitrine	Restriction digest and ligation (163/ 779)	-	AgeI and BsrGI

17	996	mTurquoise2-NES-eDHFR-Rap1Awt	QuickChange (961)	18	-
18	997	mTurquoise2-NES-eDHFR-Rap1AS17N	QuickChange (996)	19	-

8.2.3 Oligo pairs for cloning

No.	Forward primer/ Reverse primer
1	5´-AGCTGGGAGAAGACAAGCAT-3´ / 5´-CCGAAGAGATACCAGGGCAT-3´
2	5´-CATGGACGAGCTGTACAAGTCTTCCGGTTCTGGAAGTGGAATGGC TAATGAACGCATG-3´ / 5´-ATAAACAAGTTAACAACAACCTAATCTATAACTCCAACCTGAG-3´
3	5´-CATGGACGAGCTGTACAAGTCTTCCGGTTCTGGAAGTGGAGAAGT GGATCTGACCGCAC-3´ / 5´-TACACTGGATATGTGTTGGTAGATAAATGTCATAGAC-3´
4	5´-ACCAACACATATCCAGTGTAGCATCAAAC-3´ / 5´-ATAAACAAGTTAACAACAACCCAGCTCAGAAGAGAAGTC-3´
5	5´-CATGGACGAGCTGTACAAGTCTTCCGGTTCTGGAAGTGGACAGAGT GACACCCCGGAG-3´ / 5´-TACACTGGATATGTGTTGGTAGATAAATGTCATAGACTG-3´
6	5´-ACCGGCGGCATGGACGAGCTGTACAAGTCTTCCGGTTC-3´ / 5´-CTTCCAGAACCGGAAGACTTATCTATAACTCCAACCTGAG-3´
7	5´-CGCCGAGGGCCGCCACTCCACCGGCGGCATGGACGAGC-3´ / 5´-TGTACAGCTCGTCCATGCCGTATTTGTAACCATTATAAGCTGCAATA AACAAGTTAACAACAACCCAGC-3´
8	5´-GGTCGCCACCATGGTGAGCAAGGGCGAG-3´ / 5´-CGCGGCCGCTTTACTTGTACAGCTCGTCCATG-3´

9	5′-GTACAAGTAAAGCGGCCGCGACTCTAGATC-3′ / 5′-TGCTCACCATGGTGGCGACCGGTAGCGC-3′
10	5′-CGTCAGATCCGCTAGCGCTACCGGTCGCCACCATGGTG AGCAAG-3′ / 5′-TGCCCACGCCCACCGAGCCCAGCACCACCAC-3′
11	5′-GGGCTCGGTGGGCGTGGGCAAGTCCGCG-3′ / 5′-ATATTAACGCTTACAATTTACGCGTTAAGATACATTGATGAGTTTGGA CAAACCACAACTAGAATGCAG-3′
12	5′-GGTCGCCACCATGGTGAGCAAGGGCGAG-3′ / 5′-AACCGGAAGACTTGTACAGCTCGTCCATGC-3′
13	5′-GCTGTACAAGTCTTCCGGTTCTGGAAGTGGAGAAGTG-3′ / 5′-TGCTCACCATGGTGGCGACCGGTAGCGC-3′
14	5′-CTCTAGATCCATGCGTGAGTACAAGCTAG-3′ / 5′-AATTGAGTTATTCCACTGGTGTTTTCCTATTTATC-3′
15	5′-ACCAGTGGAATAACTCAATTGTTGTTGTTAAC-3′ / 5′-ACTCACGCATGGATCTAGAGGTGGATCC-3′
16	5′-CTCTAGATCCATGAGAGAGTACAAAGTGGTGGTGCTGG-3′ / 5′-AATTGAGTTAGTTGGGCTGCGCCGCGTA-3′
17	5′-GCAGCCCAACTAACTCAATTGTTGTTGTTAAC-3′ / 5′-ACTCTCTCATGGATCTAGAGGTGGATCC-3′
18	5′-GGTTCAGGAGGCGTTGGGAAGTC-3′ / 5′-CAACGCCTCCTGAACCAAGGACCAC-3′

19	5´-GGCGTTGGGAAGAATGCTCTGACA-3´ / 5´-CTGAACTGTCAGAGCATTCTTCCCAACG-3´

Eidesstattliche Versicherung (Affidavit)

Lüttig, Ricarda
Name, Vorname
(Surname, first name)

193913
Matrikel-Nr.
(Enrolment number)

Belehrung:

Wer vorsätzlich gegen eine die Täuschung über Prüfungsleistungen betreffende Regelung einer Hochschulprüfungsordnung verstößt, handelt ordnungswidrig. Die Ordnungswidrigkeit kann mit einer Geldbuße von bis zu 50.000,00 € geahndet werden. Zuständige Verwaltungsbehörde für die Verfolgung und Ahndung von Ordnungswidrigkeiten ist der Kanzler/die Kanzlerin der Technischen Universität Dortmund. Im Falle eines mehrfachen oder sonstigen schwerwiegenden Täuschungsversuches kann der Prüfling zudem exmatrikuliert werden, § 63 Abs. 5 Hochschulgesetz NRW.

Die Abgabe einer falschen Versicherung an Eides statt ist strafbar.

Wer vorsätzlich eine falsche Versicherung an Eides statt abgibt, kann mit einer Freiheitsstrafe bis zu drei Jahren oder mit Geldstrafe bestraft werden, § 156 StGB. Die fahrlässige Abgabe einer falschen Versicherung an Eides statt kann mit einer Freiheitsstrafe bis zu einem Jahr oder Geldstrafe bestraft werden, § 161 StGB.

Die oben stehende Belehrung habe ich zur Kenntnis genommen:

Official notification:

Any person who intentionally breaches any regulation of university examination regulations relating to deception in examination performance is acting improperly. This offence can be punished with a fine of up to EUR 50,000.00. The competent administrative authority for the pursuit and prosecution of offences of this type is the chancellor of the TU Dortmund University. In the case of multiple or other serious attempts at deception, the candidate can also be unenrolled, Section 63, paragraph 5 of the Universities Act of North Rhine-Westphalia.

The submission of a false affidavit is punishable.

Any person who intentionally submits a false affidavit can be punished with a prison sentence of up to three years or a fine, Section 156 of the Criminal Code. The negligent submission of a false affidavit can be punished with a prison sentence of up to one year or a fine, Section 161 of the Criminal Code.

I have taken note of the above official notification.

Dortmund, den
Ort, Datum
(Place, date)

Unterschrift
(Signature)

Titel der Dissertation:
(Title of the thesis):

Crosstalk between Rac and Rap GTPases in migrating cells

Ich versichere hiermit an Eides statt, dass ich die vorliegende Dissertation mit dem Titel selbstständig und ohne unzulässige fremde Hilfe angefertigt habe. Ich habe keine anderen als die angegebenen Quellen und Hilfsmittel benutzt sowie wörtliche und sinngemäße Zitate kenntlich gemacht.
Die Arbeit hat in gegenwärtiger oder in einer anderen Fassung weder der TU Dortmund noch einer anderen Hochschule im Zusammenhang mit einer staatlichen oder akademischen Prüfung vorgelegen.

I hereby swear that I have completed the present dissertation independently and without inadmissible external support. I have not used any sources or tools other than those indicated and have identified literal and analogous quotations.

The thesis in its current version or another version has not been presented to the TU Dortmund University or another university in connection with a state or academic examination.*

*Please be aware that solely the German version of the affidavit ("Eidesstattliche Versicherung") for the PhD thesis is the official and legally binding version.

Dortmund, den
Ort, Datum
(Place, date)

Unterschrift
(Signature)

technische universität
dortmund

Fakultät für Chemie
und Chemische Biologie

Datum: _____

An die/den Vorsitzende/n des Promotionsausschusses
der Fakultät für Chemie und Chemische Biologie der TU Dortmund

Eigenständigkeitserklärung für Dissertationen

nach der Ergänzung zur Promotionsordnung vom 29.10.2010
(Promotionsstudiengang) am 20.11.2023

Ich versichere hiermit an Eides statt, dass ich die vorliegende Dissertation mit dem folgenden Titel

Crosstalk between Rac and Rap GTPases in migrating cells

selbstständig und ohne unzulässige fremde Hilfe verfasst habe. Ich habe keine anderen als die angegebenen Quellen und Hilfsmittel benutzt sowie wörtliche und sinngemäße Zitate kenntlich gemacht. Ich erkläre zudem, dass ich beim Einsatz von Schreib- und Bildwerkzeugen, die durch Künstliche Intelligenz (KI) unterstützt werden, diese in der Übersicht verwendeter Hilfsmittel mit ihrem Produktnamen, meiner Bezugsquelle sowie der spezifischen Methodik vollständig aufgeführt habe und, bei Übernahme von durch generative Schreibwerkzeuge erstellten Texten, die betreffenden Textstellen in der Arbeit als mit KI-generierter Unterstützung verfasst gekennzeichnet habe. Die Arbeit hat in gleicher oder ähnlicher Form noch keiner Prüfungsbehörde vorgelegen. Ich habe sichergestellt, dass durch die Verwendung generativer Modelle kein fremdes geistiges Eigentum verletzt wurde und ich kein wissenschaftliches Fehlverhalten etwa in Form von Plagiaten begangen habe.

Name: Lüttig, Vorname Ricarda

Matrikelnummer: 193913

Datum, Unterschrift Dortmund, den